Spatio-Temporal Variability and Trend of Rainfall and Its Association with Pacific Ocean Sea Surface Temperature in West Harerge Zone, Eastern Ethiopia

Getachew Bayable Tiruneh (bayable.geta@gmail.com)
Bahir Dar University
Gedamu Amare
Oda Bultum University
Getnet Alemu
Oda Bultum University
Temesgen Gashaw
Bahir Dar University

Research

Keywords: CHIRPS, MK trend test, Rainfall Variability, SST, West Harerge Zone

Posted Date: November 11th, 2020

DOI: https://doi.org/10.21203/rs.3.rs-104059/v1

Version of Record: A version of this preprint was published on January 20th, 2021. See the published version at https://doi.org/10.1186/s40068-020-00216-y.

Spatio-Temporal Variability and Trend of Rainfall and Its Association with Pacific Ocean Sea Surface Temperature in West Harerge Zone, Eastern Ethiopia

Getachew Bayable[1*], Gedamu Amare[2], Getnet Alemu[3], Temesgen Gashaw[1,4]

[1]Department of Natural Resource Management, College of Agriculture and Environmental Science, Bahir Dar University, Ethiopia
[2]Institute of Land Administration, Oda Bultum University, Ethiopia
[3]Department of Environmental Science, College of Natural Resource and Environmental Science, Oda Bultum University, Ethiopia
[4]Water and Land Resource Center, Addis Ababa University, Ethiopia

*Corresponding author: bayable.geta@gmail.com

Getachew Bayable
Department of Natural Resource Management, College of Agriculture and Environmental Science, Bahir Dar University, Ethiopia
Email: bayable.geta@gmail.com

Gedamu Amare
Institute of Land Administration, Oda Bultum University, Ethiopia
Email: gedamuamare2@gmail.com

Getnet Alemu
Department of Environmental Science, College of Natural Resource and Environmental Science, Oda Bultum University, Ethiopia
Email: getneta06@gmail.com

Temesgen Gashaw
Department of Natural Resource Management, College of Agriculture and Environmental Science, Bahir Dar University, Ethiopia
Water and Land Resource Center, Addis Ababa University, Ethiopia
Email: gtemesgen114@gmail.com

Abstract

Background: Rainfall variability is a common characteristic in Ethiopia and it exceedingly affects agriculture particularly in the eastern parts of the country where rainfall is relatively scarce. Hence, understanding the spatio-temporal variability of rainfall is indispensable for planning mitigation measures during high and low rainfall seasons. This study examined the spatio-temporal variability and trends of rainfall in the West Harerge Zone, eastern Ethiopia.

Method: The coefficient of variation (CV) and standardized anomaly index (SAI) was employed to analyze rainfall variability while Mann-Kendall (MK) trend test and Sen's slop estimator were employed to examine the trend and magnitude of the rainfall changes, respectively. The association between rainfall and Pacific Ocean Sea Surface Temperature (SST) was also evaluated by the Pearson correlation coefficient (r).

Results: The annual rainfall CV ranges from 12-19.36% while the seasonal rainfall CV extends from 15-28.49%, 24-35.58%, and 38-75.9% for average *Kiremt* (June-September), *Belg* (February-May), and *Bega* (October-January) seasons, respectively (1983-2019). On the monthly basis, the trends of rainfall decreased in all months except in July, October, and November. However, the trends of rainfall were not statistically significant (α = 0.05), unlike November. The annual rainfall trends showed a non-significant decreasing trend. On a seasonal basis, the trend of mean *Kiremt* and *Belg* seasons rainfall was decreased. But, it increased in *Bega* season although it was not statistically significant. Moreover, the correlation between rainfall and Pacific Ocean SST was negative for *Kiremt* while positive for *Belg* and *Bega* seasons. Besides, the correlation between rainfall and Pacific Ocean SST was negative at annual time scales.

Conclusions: High spatial and temporal rainfall variability on monthly, seasonal, and annual time scales was observed in the study area. Seasonal rainfall has high inter-annual variability in the dry season *(Bega)* than other seasons. The trends in rainfall were decreased in most of the months. Besides, the trend of rainfall was increased annually and in the *Bega* season rather than other seasons. Generally, the occurrence

of droughts in the study area was associated with ENSO events like most other parts of Ethiopia and East Africa.

Keywords: CHIRPS; MK trend test; Rainfall Variability; SST; West Harerge Zone

1. Introduction

In recent decades, climate change and variability generate a significant impact on the environment, society, and economy globally (IPCC 2007; Chou and Lan 2012; IPCC 2012; Tierney et al. 2013; Birkmann and Mechler 2015; Wang et al. 2018). Specifically, rainfall is one of the major climatic variables that affect both the spatial and temporal patterns of water availability for agriculture, industry, food security, hydropower water supply, and energy balance (De Luís et al. 2000; Zhang et al. 2010; Conway and Schipper 2011; Zhang et al. 2011; Elliott et al. 2014; Ganguly et al. 2015; Pal et al. 2017; Ayehu et al. 2018; Weldegerima et al. 2018). In many African countries, more than 85% of the population is engaged in rain-fed agriculture (Diro et al. 2011; Mulugeta et al. 2019). Due to this, they are exceedingly susceptible to anomalously high and/or low rainfall amounts (Anyah and Qiu 2012; IPCC 2014; IPCC 2018).

In East Africa, rainfall is characterized by its inter-annual variability, which has contributed to the shocking droughts and floods; affecting the lives of many people (Cheung et al. 2008; Mekasha et al. 2014; Viste et al. 2013; Omondi et al. 2014; Tierney et al. 2015). Ethiopia is known for its high rainfall variability across space and time due to geographical location and topographic complexity (Gemechu 1988; Mengistu et al. 2014; Worku 2015). In Ethiopia, spatial variations can be characterized by the rainfall seasonal cycle, amount, onset, and cessation times, and length of growing season (Segele and Lamb 2005). Moreover, rainfall can be temporally varied from days to decades in terms of the direction and magnitude of rainfall trends over regions and seasons (Jury and Funk 2013; Viste and Sorteberg 2013; Worku et al. 2019). Reliable and appropriate seasonal rainfall trend analysis and rainfall forecasts are crucial for mitigation of rainfall related disasters (Diro et al. 2011).

Analysis of spatiotemporal variability of rainfall is vital for water resource management, agricultural production, and climate change mitigation (Ayalew et al. 2012; Zhao et al. 2015). For this purpose, it requires consistent and spatially well-distributed long-term meteorological station records. The distributions of meteorological stations in developing countries in general and in Ethiopia, in particular, are scarce, unevenly distributed, have poor data quality and data discontinuities (Katsanos et al. 2016; Kimani et al. 2017; Fenta et al. 2018). These are also the limitations of meteorological stations in the West Harerge zone. To overcome these problems, long-term satellite-based rainfall estimates have become vital sources of rainfall data for sparse regions (Ayehu et al. 2018; Cattani et al. 2018; Dinku et al. 2018; Fenta et al. 2018; Alemu and Bawoke 2019).

Currently, understanding the spatial-seasonal variations of rainfall and its association with SST is very crucial to produce reliable weather and climate forecasts for users (Degefu et al. 2017). Previous studies showed that El Niño/Southern Oscillation (ENSO) has a great influence on the inter-annual rainfall variability in Ethiopia (Camberlin et al. 2001; Gissila et al. 2004; Lyon 2014; Seneshaw and Yitea 2015; Alhamshry et al. 2020). During El Niño (La Niña), precipitation in equatorial east Africa might be positively or negatively affected by easterly (westerly) wind anomalies (Ratnam et al. 2014). ENSO is the inter-annual fluctuation of the atmosphere-ocean system in the equatorial Pacific and it has three phases: warm (El Niño), cold (La Niña), and Neutral (Chen et al. 2014; Yu et al. 2015; Jajcay et al. 2018; FAO 2019). Neutral conditions occur when neither El Niño nor La Niña is present (FAO 2019). El Niño is a recurrent global atmospheric oceanic phenomenon associated with an increase in SST in the central tropical Pacific Ocean. It boosts the risk of heavy rainfall and flooding in some parts of the world and the risk of drought in some parts (FAO 2019). The SST of the tropical Pacific shows a discrepancy both spatially and temporally (Philip 2018) and a very high correlation exists between precipitation and SST (Pegion and Kirtman 2008; Wu et al. 2008; Chen et al. 2014).

Several studies have been conducted on spatio-temporal variability and trends of rainfall in Ethiopia (Degefu and Bewket 2013; Gummadi et al. 2017; Gedefaw et al. 2018; Mohammed et al. 2018; Moloro 2018; Weldegerima et al. 2018; Abegaz and Mekoya 2020; Geremew et al. 2020). Although different studies have been conducted on the Spatio-temporal variability and trends of rainfall in Ethiopia, there are limitations in the West Harerge Zone. West Harerge Zone is one of the most droughts prone areas of Ethiopia due to variations of rainfall intensity which can be linked to ENSO. Hence, the objective of this study was to investigate the spatio-temporal variability and trends of rainfall and its association with Pacific Ocean SST in the West Harerge Zone of eastern Ethiopia. The findings from this study would be vital for future planning and development measures such as flood control and protection; drought monitoring and early warning systems.

2. Materials and Methods

2.1 Description of the study area

The study area, West Harerge Zone, is located in eastern Ethiopia, approximately between 7° 51'- 9° 28' N and 40° 01' - 41° 34'E (Fig 1). It covers a total area of 1689497.6 ha of land (Wondosen 2017) and its elevation ranges from 603 - 3075 m a.s.l (Fig 1). Based on the traditional agroecological classifications of Ethiopia, the study area is categorized into three zones. These are tropical (500-1500 m), sub-tropical (1500-2300 m), and temperate (2300-3200 m) (OWWDSE 2010). There are two rainy seasons in this area, the main rainy season (*Kiremt)* spans from June to September, and the short rainy season (*Belg)* which extends from February to May. It has the mean monthly rainfall and an average temperature of 67.8 mm and 17.5 to 27.5°C, respectively (MOA 2000).

Fig 1: Location Map of the study area

2.2 Data types and sources

SST and rainfall data have been obtained from different sources. Time series monthly Pacific Ocean SST data (1984-2018) in the NINO3.4 region were downloaded from the National Oceanic and Atmospheric Administration (NOAA) satellite mission website (http://www.cgd.ucar.edu/cas/catalog/climind/TNI_N34/index.html). The NINO3.4 index mean SST was calculated by taking the spatial average SST within the NINO3.4 region, which extends from 5°N to 5° S latitude and from 120°W to 170° W longitude (in the Pacific Ocean) (Loua et al. 2019; Yin et al. 2020). According to Babu (2009) and Zaroug (2010), NINO 3.4 SST data has characteristics of both NINO3 and NINO4. Accordingly, the Pacific Ocean SST of the NINO3.4 region was used in this study.

Rainfall data were collected from remote sensing satellite estimates. Most rainfall data from in-situ meteorological stations had short period records and a large percentage of missing data problems (1983-2019). Moreover, the spatial distributions of stations were scarce and not evenly dispersed in the study area. In this case, Climate Hazards Group Infra-Red Precipitation with Stations (CHIRPS) satellite rainfall data (https://data.chc.ucsb.edu/products/CHIRPS-2.0/) are a vital source of rainfall data (Asfaw et al. 2018; Dinku et al. 2018; Belay et al. 2019). CHIRPS is a quasi-global dataset (covering the area between 50° N and 50° S) available from 1981 to present-day at 0.05° spatial resolution (~ 5.3 km) and it is produced using multiple data sources (Funk et al. 2015). In-situ meteorological station data for Asebe Teferi, Hirna, Bedesa, Gelemso, Meiso, Asebot, and Kora from the National Meteorological Agency (NMA) of Ethiopia were used as a reference to evaluate the accuracy of the CHIRPS satellite rainfall product in the West Harerge Zone. Missing values were handled by taking the average of the preceding and succeeding months for monthly missed data but years with missed data were excluded from analysis in the station data (Traore et al. 2014; Asfaw et al. 2018).

Table 1: Characteristics of in-situ meteorological stations and percentage of missing data

2.3 Validation of CHIRPS rainfall data

Satellite-based rainfall estimates provide well timed, repetitive, and cost-effective information at different time scales (Toté et al. 2015; Muthoni et al. 2019). However, they show different uncertainties with techniques. These may arise from relative algorithm errors, spatiotemporal sampling errors, and satellite instruments themselves (Gebremichael et al. 2005; Fenta et al. 2018; Alemu and Bawoke 2019; Belay et al. 2019). These may affect the accuracy and may result in a significant error when used for different applications. Due to this, the validation of satellite rainfall data is required at different spatial and temporal scales (Dinku et al. 2007; Ayehu et al. 2018; Dinku et al. 2018). Evaluation and comparison between different satellite rainfall data have been shown in east Africa, including in different parts of Ethiopia (Dinku et al. 2007; Dinku et al. 2014; Ayehu et al. 2018; Dinku et al. 2018; Fenta et al. 2018) and the results show that the CHIRPS product performs better than most long-term satellite rainfall products. The CHIRPS data product is developed by the United States Geological Survey (USGS) and the Climate Hazards Group (CHG) at the University of California (Knapp et al. 2011; Funk et al. 2015).

Validation of the CHIRPS satellite rainfall data was performed at monthly, seasonal, and annual time scales for Asebe Teferi, Asebot, Bedesa, Hirna, Gelemso, Meiso, and Kora locations with the corresponding meteorological gauge station data. The performance of CHIRPS rainfall data was assessed using different statistics (Table 2) (Dinku et al. 2007; Dinku et al. 2018; Larbi et al. 2018; Goshime et al. 2019). Root mean square error (RMSE) (ranges from 0 to ∞), mean bias error (MBE) (ranges from-∞ to ∞) and mean absolute error (MAE) (ranges from 0 to ∞) measures the average magnitude of estimation error and the perfect score for these statistics is zero. Positive and negative MBE value indicates an overestimation and underestimation of CHIRPS data products, respectively (Fenta et al. 2018). Pearson Correlation Coefficient (r) measures the strength of the linear relationship between CHIRPS and meteorological station rainfall data (Alemu and Bawoke 2019) and ranges from a negative one to a positive one. The Nash–Sutcliff efficacy Coefficient (NSE) describes the relative magnitude of the variance of the residuals compared to the variance of the observed values of precipitation (Nash and Sutcliffe 1970) and it ranges from -∞ to one. The higher value of NSE shows a better agreement between the CHIRPS satellite rainfall and meteorological gauge station data. In contrast, negative values indicate that the meteorological station is a better estimate and zero indicates that the meteorological station is as good as the CHIRPS rainfall products.

Table 2: Statistical indicators, equation, range, and best value used in the study

2.4 Spatio-temporal variability and trend analysis of rainfall

The coefficient of variation (CV) and standardized anomaly index (SAI) was computed to analyze the temporal variability of rainfall.

i. Coefficient of Variation (CV)

Spatiotemporal variability of annual, seasonal, and monthly rainfall for each pixel was examined by calculating the coefficient of variation (CV) (Muthoni et al. 2019). CV was computed as:

$$CV(\%) = \left(\frac{\sigma}{\bar{x}}\right) 100 \tag{1}$$

where CV is the coefficient of variation of rainfall, σ is the standard deviation of rainfall and $\bar{x}$ is long term mean of rainfall.

ii. Standardized Anomaly Index (SAI)

Standardized anomaly index (SAI) was used as a descriptor of rainfall variability and it indicates the number of standard deviations that a rainfall event deviates from the average of the considered years (Funk et al. 2015). It was also used to determine the frequency of dry and wet years in the record and used to assess the frequency and severity of droughts (Alemu and Bawoke 2019). It indicates the departure from long term mean with negative values representing periods of below-normal rains (droughts) while positive values reflect above normal rains (flood risk) (Muthoni et al. 2019). SAI value is classified as extremely wet (SAI>2), very wet (1.5 ≤ SAI ≤1.99), moderately wet (1 ≤ SAI ≤1.49), near normal (- 0.99 ≤ SAI ≤ 0.99), moderately dry (-1.49 ≤ SAI ≤ -1), severely dry (-1.99 ≤ SAI ≤ -1.5) and extremely dry (SAI≤ -2) (McKee et al. 1993; Funk et al. 2015) and it is computed using the following equation:

$$SAIi = \frac{Xi - \bar{x}}{\sigma} \tag{2}$$

Where $\boldsymbol{SAIi}$ ***is*** the standardized anomaly index in year i, Xi is the rainfall value in a year i**;** $\bar{\boldsymbol{x}}$ is the long-term mean of rainfall and $\boldsymbol{\sigma}$ is the standard deviation of rainfall.

iii. Mann-Kendall Trend Test and Sen's Slope Estimator

The Mann-Kendall (MK) trend test (Non-parametric statistical test) and Sen's Slope estimator was employed to evaluate the trends and magnitudes of rainfall changes using XLSTAT 2020. MK trend test is one of the most commonly used and preferred nonparametric tests for finding trends in time series hydroclimate(Gocic and Trajkovic 2013; Ahmed et al. 2014; Feng et al. 2016). This method is less affected by missing values and uneven data distribution, and it is less sensitive to outliers because it considers ranks of the observations rather than their actual values (Kendall 1975; Yue et al. 2002; Poudel and Shaw 2016; Belay et al. 2019). Therefore, the World Meteorological Organization strongly recommends the MK trend test for general use in trend analysis (Mitchell et al. 1966). It is used to confirm whether there is a statistically significant or insignificant trend in rainfall variability (Jain and Kumar 2012).

According to the MK test, the null hypothesis (H_0) of no trend, that is the observations Yi are randomly ordered in time, against the alternative hypothesis (H_1), where there is a monotonic (increasing or decreasing) trend in the time series was tested. Based on (Mann 1945; Kendall 1975; Yue et al. 2002) the MK statistics S is computed using the following formula;

$$S = \sum_{i=1}^{n-1} \sum_{j=i+1}^{n} \mathrm{Sign}(yj - yi) \tag{3}$$

where Yi and Yj are sequential data values for the time series data of length n and

$$\mathrm{Sign}(yj - yi) = \begin{cases} 1 \text{ if } (yj - yi) > 0 \\ 0 \text{ if } (yj - yi) = 0 \\ -1 \text{ if } (yj - yi) < 0 \end{cases} \tag{4}$$

If the dataset is identically and independently distributed, then the mean of S is zero and the variance of S is given by

$$\mathrm{Var}(S) = \frac{1}{18}\left[n(n-1)(2n+5) - \sum_{i=0}^{m} ti(ti-1)(2ti+5)\right] \tag{5}$$

where n is the length of the dataset, m is the number of tied groups (a tied group is a set of sample data having the same value) in the time series and ti is the number of data points in the i^{th} group

The Z statistics are calculated using the formula

$$Z=\begin{cases} \frac{S+1}{\sqrt{Var\ (S)}} \text{ for } S < 0 \\ 0 \quad \text{ for } S = 0 \\ \frac{S-1}{\sqrt{Var\ (S)}} \text{ for } S > 0 \end{cases} \tag{6}$$

A significance level α = 0.05 was used to test either an upward or downward monotone trend. The decision for the two-tail test was made by comparing the computed Z with critical values. The null hypothesis is rejected when the absolute value of computed Z is greater than the critical values or the p-value is less than the selected significance level (α = 0.05 or 0.1). Furthermore, when the null hypothesis is rejected, the direction of trends is upward for positive Z-value and downward for negative Z-value (Hamlaoui-Moulai et al. 2013). If the null hypothesis is rejected, the result was said to be statistically significant.

Likewise, to assess the relative strength of the MK trend test in time series data, the rate of change of the trend has been determined using Sen's (1968) slope estimator. As stated by Jain and Kumar (2012), Sen's slope estimates are commonly used to determine the magnitude of trends in hydro-climate time series. It limits the influence of missing values or outliers on the slope in comparison with linear regression (Bouza-Deaño et al. 2008; Alemu and Bawoke 2019; Mekonen et al. 2020). The magnitude of the monotonic trend in hydrologic time series was calculated by using the nonparametric Sen's estimator of the slope using the following equation (Sen 1968).

$$\beta = \text{median}\left(\frac{yj-yi}{j-i}\right) \tag{7}$$

where β represents the median value of the slope values between data measurements yi and yj at the time steps i and j (i < j), respectively. The positive value of β indicates an increasing trend whereas the negative value of β indicates a decreasing trend. The sign of β reflects data trend direction, whereas its value indicates the steepness of the trend (Alemu and Bawoke 2019).

2.5. Correlation Analysis of the Rainfall and SST

The Pearson correlation coefficient (r) reflects the degree and direction of the relationship between two variables (Guo et al. 2014; Qian et al. 2016; Tiruneh et al. 2018). In this study, the Pearson correlation coefficient (r) was employed to test the association between rainfall and SST. A larger absolute value of r indicates a stronger correlation between the two variables (Qian et al. 2016; Tiruneh et al. 2018). The absolute value of r was divided into a weak correlation ($0 < |r| \leqslant 0.3$), a low correlation ($0.3 < |r| \leqslant 0.5$), a moderate correlation ($0.5 < |r| \leqslant 0.8$), and a strong correlation ($0.8 < |r| \leqslant 1$) (Li et al. 2014). Pearson correlation coefficients were calculated using the following equation (Mu et al. 2013):

$$r = \frac{\sum_{i=1}^{n}(Xi-\overline{X})(Yi-\overline{Y})}{\sqrt{\sum_{i=1}^{n}(Xi-\overline{X})^2 \sum_{i=1}^{n}(Yi-\overline{Y})^2}} \tag{8}$$

where r is the correlation coefficient, n is the length of the time series, and i is the number of years during the analyzed periods (1984-2018). Xi and Yi are the rainfall and the SST in the year i, respectively, and $\overline{X}$ and $\overline{Y}$ are the mean rainfall and the mean of SST, respectively during the studied periods.

3. Results and Discussion

3.1 Validation of CHIRPS Rainfall Data

Validation of CHIRPS rainfall data was undertaken at the monthly, seasonal, and annual time scales using meteorological gauge stations data. The results of the validation of CHIRPS rainfall data using meteorological gauge stations data are presented in Table 3. The results of the comparison between the CHIRPS rainfall data and the meteorological gauge station rainfall data at monthly time scales in reproducing the current rainfall pattern of Asebe Teferi, Hirna, Bedesa, Gelemso, Meiso, Asebot, and Kora stations location was shown in Fig 2. A very good agreement was observed between meteorological gauge stations data and CHIRPS rainfall data on a monthly time scale. The r values were ranging between 0.91- 0.99, and NSE values ranging between 0.82-0.98 for all station locations (Table 3). As compared to the monthly rainfall data, MAE, MBE, and RMSE values showed good performance of CHIRPS rainfall estimates in the West Harerge Zone (Table 3). Monthly CHIRPS rainfall products were underestimated by about 1.2 mm, 2.5 mm, 5.3 mm, and 11.4 mm for Meiso, Hirna, Asebot, and Bedesa locations, respectively. On the other hand, monthly CHIRPS rainfall data was overestimated at Gelemso, Asebe Teferi, and Kora locations about 2.9 mm, 3.1 mm, and 10.1 mm, respectively. Based on the statistical measures monthly CHIRPS rainfall products perform better at Hirna and Meiso locations (Table 3) than other station locations. Overall, monthly rainfall data extracted from CHIRPS products were strongly correlated with the rainfall data for selected gauge stations. This indicates that the performance of the monthly CHIRPS rainfall product is well in the study area. The findings of this study agreed with a study carried out by Saeidizand et al. (2018) in Iran; Larbi et al. (2018) in the Vea catchment of Ghana; Alemu and Bawoke (2019) in the Amhara regions of Ethiopia and Atiah et al. (2019) in Ghana.

Besides, CHIRPS rainfall for *Bega* (October - January) season showed good correspondence with gauge with r values ranging between 0.45 and 0.95, and NSE values between 0.21 and 0.87 for all station locations. Similarly, CHIRPS rainfall data in the *Belg* season showed a very high agreement with the gauge station data with r values between 0.68 and 0.89, and NSE values ranging between 0.26 and 0.74 for all station locations. In *Kiremt* season, good agreement was observed with the gauge station data for Asebe Teferi, Bedesa, Gelemso, and Meiso station locations whereas the correlation coefficient is weak for Asebot (r = 0.26), Hirna (r = 0.32), and Kora (r = 0.36) station locations. The MAE was small for most of the station locations relative to the gauge rainfall data in all seasons. This indicates CHIRPS rainfall data was comparable to the gauge rainfall data in the study area. The result of this study was also supported by Saeidizand et al. (2018) and revealed that the presence of a good agreement between CHIRPS and gauge stations rainfall data in Iran during *Belg*, *Bega,* and *Kiremt* seasons. In the *Bega* season, CHIRPS rainfall data were overestimated at Asebe Teferi, Gelemso, Hirna, and Kora station locations whereas CHIRPS was underestimated at Asebot, Bedesa, and Meiso station locations in the study area. Similarly in *Belg* season, CHIRPS rainfall data were overestimated at Kora and Meiso station locations, while underestimated at Asebot, Bedesa, Asebe Teferi, Gelemso, and Hirna station locations. CHIRPS rainfall data was also overestimated at Kora and Gelemso station locations and underestimated at Asebot, Bedesa, Asebe Teferi, Meiso, and Hirna station locations during *Kiremt* season (Table 3).

At the annual time scale, a good agreement with the gauge station data was also observed with r values between 0.56 and 0.81 and NSE values between 0.04 and 0.59 for all station locations, except Asebot (r = 0.37) and Hirna (r = 0.4). The MBE, MAE, and RMSE for Asebot and Hirna station locations were small relative to the gauge station rainfall (Table 3) and it was comparable to the gauge station data in the study area. At annual time scales, CHIRPS rainfall data was underestimated at Asebot, Bedesa, Asebe Teferi, Meiso, and at Hirna station locations, while overestimated at Kora and Gelemso station locations. Generally, as compared to previous studies (Ayehu et al. 2018; Dinku et al. 2018; Fenta et al. 2018; Alemu and Bawoke 2019) the CHIRPS rainfall products perform well for the West Harerge Zone.

Table 3: Mean monthly, seasonal, and annual time scale statistical analysis of rainfall for the meteorological station and CHIRPS rainfall data

Fig 2: Performance evaluation of CHIRPS rainfall with meteorological station rainfall based on the mean monthly rainfall in the West Harerge Zone

3.2 Distribution of Rainfall

Long-term mean annual CHIRPS rainfall estimates (1983-2019) ranged between 528.913 and 1214.75 mm (Fig 3b, c). This shows high spatial variability of rainfall over the area. The highest rainfall values were observed in the western, central, and northeastern parts of the study area. On the other hand, the lowest rainfall values were observed in the southeastern and northwestern parts of the study area. The highest annual rainfall values (996-1214.75 mm) were recorded around Tulo, Goba Koricha, the northern part of Habro, the northeastern part of Mesela, southwestern part of Chiro Zuria district, the southeastern part of Anchar, and Doba district (Fig 3b). Meiso and the southeastern part of the Boke district received the lowest annual rainfall amount (528-706 mm). The highest annual rainfall values were observed in the highest elevation area and the lowest rainfall value was recorded in the lowest elevation area (Fig 3a, b). The finding of this study is supported by Belay et al. (2019), who reported that mean annual rainfall and elevations are highly correlated in the Beles Basin of Ethiopia.

Fig 3: Elevation (a), spatial distributions of long-term mean annual rainfall (mm) across the district (b) and spatial distributions of long-term mean annual rainfall (c) of West Harerge Zone (1983-2019)

The spatial distribution of rainfall for all seasons (1983-2019) is shown below (Fig 4a, b, c). During the *Bega* season, the southern and central parts of the study area received maximum rainfall value while the northern part received the lowest rainfall value. Similarly, during *Belg*, the highest rainfall values were observed in the southern, central, and northeastern parts, whereas the lowest rainfall values were recorded in northern and northwestern parts of the study area. During *Kiremt*, the highest rainfall values were recorded in the western, central, and northeastern parts while the lowest rainfall values were recorded in the southeastern and northwestern parts of the study area. *Kiremt* season rainfall was almost followed the same spatial distribution as that of the annual rainfall. Furthermore, in this season rainfall and elevation were highly correlated.

Fig 4: Spatial distributions of mean average *Kiremt* rainfall (mm) (a) mean average *Belg* rainfall (mm) (b) and mean average *Bega* rainfall (mm) (c) of the West Harerge Zone (1983-2019)

Long-term mean monthly rainfall (1983-2019) is shown in Fig 5 and 6. It revealed that April, May, July, August, and September was the wettest months, while January, February, November, and December were the driest months. Little rainfall was recorded in March, June, and October months. Belay et al. (2019) also find that June, July, August, and September was the main rainy months, and November, December, January, February, and March was the driest months in the Beles Basin of Ethiopia. The highest value of rainfall was recorded in the August and September months, while the lowest value of rainfall was recorded in January month (Fig 6).

Fig 5: Mean monthly rainfall of West Harerge Zone (1983-2019)
Fig 6: Spatial distributions of mean monthly rainfall of West Harerge Zone (1983-2019)

3.3 Spatio-Temporal Variability and Trend of Rainfall in West Harerge Zone

3.3.1 Spatio-Temporal Variability of Rainfall

The CV result calculated for each pixel (1983-2019) in the study area is shown in Fig 7. Relatively highest inter-annual variability (CV>17%) was observed in the southern, northern, and southeastern parts of the study area. In contrast, less inter-annual variability (CV<13%) was observed in the western and northeastern parts of the area (Fig 7). The highest inter-annual variability was experienced in the northern part of Meiso, southeastern parts of Hawi Gudina, Boke, and Kuni district, and it reflects that there is greater contrast in annual rainfall values from year to year. Inter-annual variability of rainfall and mean annual rainfall amounts are almost inversely related (Fig 7). The findings of this study agreed with a study conducted by Dawit et al. (2019) and Yasuda et al. (2018) that revealed the inverse relationship between rainfall variability and mean annual rainfall in the Guna Tana Watershed, Upper Blue Nile Basin of Ethiopia and in the central Nile Basin, respectively. The areas with low mean annual rainfall show high inter-annual variability in the study area.

Fig 7: Spatial distribution of CV (%) of annual rainfall in West Harerge Zone (1983-2019)

The spatial distributions of the CV of seasonal rainfall in the study area are shown below (Fig 8a, b, and c). As compared to annual rainfall, seasonal rainfall had high inter-annual variability up to 75.9% with *Bega* rainfall. Besides, the CV in *Kiremt* rainfall (15% < CV<28.5%) appeared relatively stable compared to the remaining seasons. The `CV of *Belg* rainfall (24% <CV<35.58%) was higher than *Kiremt* rainfall and it indicates high inter-annual variability of *Belg* rainfall than *Kiremt* rainfall (Fig 8a, b). The result of this study agreed with the findings of Seleshi and Camberlin (2006); Ayalew et al. (2012); Taye and Zewdu (2012); Kassie et al. (2013); Viste et al. (2013); Alemayehu and Bewket (2017); Asfaw et al. (2018); Mohammed et al. (2018); Alemu and Bawoke (2019) and Geremew et al. (2020) in different parts of Ethiopia and reported that less variability of rainfall was observed in *Kiremt* season than other seasons. Similarly, Panthi et al. (2015) reported that less variability of rainfall was observed in the *Kiremt* season than other seasons in the Gandaki River Basin of Nepal Himalaya. Moreover, this result is supported by Abegaz and Mekoya (2020) and reported the *Belg* season rainfall was more variable than *Kiremt* season rainfall in the North Shewa zone of Ethiopia. The maximum CV in *Kiremt* rainfall was observed in the southern part of the study area. On the other hand, the maximum CV in the *Bega* season was observed in the northern part of the study area. Similarly, the highest values of the CV in *the Belg* season were recorded predominantly in the northern and southeastern parts of the study area.

Fig 8: Spatial distribution of CV (%) of *Kiremt* (a), *Belg* (b), and *Bega (c)* season rainfall in West Harerge Zone (1983-2019)

The spatial distribution of monthly rainfall CV (%) of the study area is shown in Fig 9. The highest inter-monthly variability (CV > 100%) was observed in January, February, October, and November months. In contrast, less inter-monthly variability (CV < 30%) was observed in some parts of June, July, August, and September months of the study area. The result of this study agreed with a study made by Belay et al. (2019), reported a small CV in June, July, August, and September months in the Beles Basin of Ethiopia.

Fig 9: Spatial distribution of monthly rainfall CV (%) of West Harerge Zone (1983-2019)

The annual rainfall anomaly (1983-2019) over the study area is shown in Fig 10 a. The rainfall anomalies showed the presence of inter-annual variability of rainfall and the percentages of negative and positive anomalies were 56.76% and 43.24%, respectively. The highest positive anomaly (2.50) was observed in the year 1983 whereas the highest negative anomaly (2.36) was observed in the year 2015. Negative anomalies pronounced particularly in 1984, 1986-1988, 1991, 1999-2005, 2008/2009, 2011/2012, 2015/2016, and in 2017, and which correspond to the historical drought years in Ethiopia (Fig 10 a). Similar findings were reported by Suryabhagavan (2017); Asfaw et al. (2018) and Alemu and Bawoke (2019) in Ethiopia. The result of this study also agree with the finding of Gebrehiwot and VanDerVeen (2013) and reported that years like 1984, 1987, 1991, 2000, 2002, 2003, and 2004 were drought years in the northern parts of Ethiopia. Furthermore, the results of the SAI analysis of seasonal rainfall of the study area (1983-2019) are shown in Fig 10 b, c, and d. The percentage of negative anomalies was larger than positive anomalies in all seasons. A Study conducted by Alemu and Bawoke (2019) stated that the percentage of negative anomalies exceeded that of positive anomalies in all seasons except *Kiremt* in the Amhara region. Similar to annual rainfall, inter-annual variability of rainfall was observed in *Belg*, *Kiremt*, and the *Bega* with negative anomalies in 59.46%, 54.05%, and 62.16% of the studied years, respectively. The highest positive anomaly was observed in the years 1983, 2010, and 1997 in *Kiremt*, *Belg*, and *Bega* seasons, respectively. On the other hand, the highest negative anomaly was observed in the year 2015, 2009, and 2010 in *Kiremt*, *Belg*, and *Bega* seasons, respectively.

Fig 10: Annual rainfall standardized anomaly index (a), mean *Kiremt* rainfall standardized anomaly index (b), mean *Belg* rainfall standardized anomaly index(c), and mean *Bega* rainfall standardized anomaly index (d) of West Harerge Zone (1983-2019)

3.3.2 Trend Analysis of Rainfall

The result of monthly rainfall MK trend-test analysis of the study area is shown in Table 4. The result showed that there was a decreased trend in January, February, March, April, May, June, August, September, and December months (1983-2019). On the other hand, there was an increasing trend in July, October, and November months (Table 4). However, the trends were not significant at a significance level of $\alpha = 0.05$ in all months except November (1983-2019). The finding of this study agreed with a study conducted by Alemu and Bawoke (2019) and reported that insignificant trends in all months except November in the Amhara region (1981-2017). Alemu and Bawoke (2019) reported a significant increasing trend in November. Similar findings were also reported by Tesfamariam et al. (2019) for all months of rainfall in Awasa, Arbaminch, and Kulunsa stations of the Rift Valley Lakes Basin of Ethiopia unlike a significant increasing trend of rainfall was observed in November for the Konso station.

Table 4: MK trend analysis of spatial average monthly rainfall in West Harerge Zone (1983-2019) at a significance level of $\alpha= 0.05$

Mean seasonal rainfall showed a downward trend in *Kiremt* and *Belg* seasons, whereas there was an upward trend in the *Bega* season (Table 5 and Fig 11b, c, and d). However, these increased and decreased trend was not significant at $\alpha = 0.05$ in mean *Bega*, *Belg*, and *Kiremt* rainfall (1983-2019) of the West Harerge Zone. Moreover, mean annual rainfall showed a downward trend (Table 5 and Fig 11a) and this downward trend is not significant at a significant level $\alpha= 0.05$. The findings of this study agreed with a study carried out by Viste et al. (2013) in southern Ethiopia and reported a declining trend of rainfall during *Kiremt*, and *Belg* season over different periods. Mulugeta et al. (2019) reported that an insignificant decreasing trend of annual rainfall in the Awash River Basin in the period (1902-2016). Gebrechorkos et al. (2019) reported that a non-significant decreasing (increasing) trend in rainfall in eastern (western) parts of Ethiopia during the *Kiremt* season from 1981 to 2016. Gebrechorkos et al. (2019) also find that an insignificant increasing trend in large parts of Eastern Africa during the *Belg* season. Similarly, Mulugeta et al. (2019) reported an insignificant increasing trend of *Belg* and *Bega* season rainfall in the Awash Basin. Weldegerima et al. (2018) find an insignificant increasing trend in both seasonal and annual timescales in the Lake Tana Basin. Moreover, Alemu and Bawoke (2019) find an insignificant increasing trend in the annual and *Kiremt* while an insignificant decreasing trend during the *Bega* season (1981-2017) in the Amhara region of Ethiopia. In contrast, Wagesho et al. (2013) and Mulugeta et al. (2019) find a significantly decreased trend in *Kiremt* rainfall (at $\alpha = 0.1$) over most parts of the Awash River Basin. Similarly, Cheung et al. (2008) find a significant decline trend of rainfall in the southwestern and central parts of Ethiopia during the *Kiremt* season. Addisu et al. (2015) find a significant decreasing trend of rainfall in DebreTabor, Zeghie, Hamusit, Yifag, and Maksegnit stations of Lake Tana Basin at an annual time scale. Degefu and Bewket (2014) reported an increasing trend in annual rainfall over several locations in the Omo-Ghibe River Basin. Meze-Hausken (2004) reported an increased rainfall trend in the northern and northeastern parts of Ethiopia. Mohammed et al. (2018) also reported that the rainfall significantly increased in *Kiremt* at Dessie, Haik, and Mekaneselam out of six meteorological stations and a decline in *Belg* at all studied stations in the South Wollo zone (1984-2014). Besides, Geremew et al. (2020) reported that the annual rainfall showed an increasing trend at all stations in Enebsiesar Midir District, northwest Ethiopia except at Mertu Lemariam during the 1987-2016 periods.

Table 5: MK trend analysis of areal average annual and mean seasonal rainfall (1983-2019) in West Harerge Zone at a significance level of α= 0.05

Fig 11: Long-term mean annual and mean average seasonal rainfall (annual (a), *Kiremt* (b), *Belg*(c) and *Bega* (d)) of West Harerge Zone (1983-2019)

3.4 Associations between Rainfall and Pacific Ocean Sea Surface Temperature (SST)

The correlation between mean *Kiremt* rainfall and NINO 3.4 SST was negative and statistically significant at a 5% significance level (Table 6). On the other hand, the correlation between mean values of rainfall and NINO 3.4 SST was generally positive in *Belg* and *Bega* seasons (Table 6). This implies that SST decreased the amount of rainfall in the *Kiremt* season and increased in *Belg* and *Bega* season across the study area over the last 35 years (1984-2018). Similarly, the correlation between mean annual rainfall and NINO3.4 SST was negative in the study area. Studies conducted by Gissila et al. (2004) and Korecha and Barnston (2007) showed the existence of a relationship between Ethiopian rainfall and equatorial Pacific SST. Tiruneh et al. (2018) revealed that the correlation between SST anomalies and rainfall was negative and positive in *Kiremt* and *Belg* seasons, respectively in the Upper Awash basin. Similarly, the negative association between mean annual rainfall and mean annual SST anomaly was also reported in the Upper Awash basin. Diro et al. (2010) showed that the equatorial Pacific SST shows a negative correlation with rainfall in various parts of Ethiopia during the *Kiremt* season. Moreover, an empirical study conducted by Seleshi and Camberlin (2006) revealed that warm ENSO periods (El Niño years) are typically associated with lower rainfall and drought years. In contrast, cold periods (La Niña years) are associated with higher rainfall amounts. The highest negative rainfall anomaly and the highest positive SST anomaly correspond to severe drought years (Seleshi and Camberlin 2006). The historical droughts in Ethiopia had been associated with ENSO events in the past (Shanko and Camberlin 1998; Fekadu 2015). The drought years in Ethiopia include 1984, 1987, 1991–1992, 1993–94, 2002, 2009, 2012, 2015/16 (Asfaw et al. 2018; Mekonen et al. 2020) either coincide or follow El Niño events shortly (Asfaw et al. 2018). The finding of this study also agreed with the above result and the rainfall anomalies for these drought periods were very low whereas the SST anomalies were very high (Fig 12). La Nina decreases the amount of rainfall in the *Belg* season unlike in the *Kiremit* season, while El Nino increases the amount of rainfall in the *Belg* season and decreases the amount of rainfall in the *Kiremt* season (1974-2013) in Bilate River Basin, Ethiopia (Moloro 2018). Weldegerima et al. (2018) reported that the rainfall was affected by the SST variations in the Lake Tana basin of Ethiopia. Besides, Wagesho et al. (2013) and Yasuda et al. (2018) reported that the inter-annual variability of rainfall in East Africa was linked with the impact of Pacific Ocean SST.

Table 6: Correlation Coefficients between Rainfall and SST (1984-2018) in West Harerge Zone

Fig 12: Association between annual rainfall anomaly and SST anomaly (a), *Kiremt* rainfall anomaly and SST anomaly (b), *Belg* rainfall anomaly and SST anomaly (c) and *Bega* rainfall anomaly and SST anomaly (d)

4. Conclusions

This study has investigated the spatiotemporal variability and trends of rainfall and its association with Pacific Ocean SST in the West Harerge Zone of eastern Ethiopia using CHIRPS rainfall products and Pacific Ocean SST data. High spatial and temporal rainfall variability on monthly, seasonal, and annual time scales was observed across the study area. The seasonal rainfall showed high inter-annual variability in the dry season *(Bega)* than other seasons. Similarly, short rainy season (*Belg)* rainfall showed high inter-annual variability than the main rainy season (*Kiremt).* The trends of rainfall were decreased but not statistically significant in most of the months during the studied periods (1983-2019). In contrast, the trend of rainfall was increased insignificantly in July and October months. However, the trend of rainfall was increased significantly in November month. Besides, the trend of rainfall was increased annually and in *the Bega* season rather than other seasons. But, the trends of rainfall were not significant at a 5% significance level. Besides, NINO 3.4 SST showed a decreasing effect on the amount of rainfall in the *Kiremt* season and an increasing effect on the amount of rainfall in *Belg* and *Bega* season across the study area. Likewise, equatorial Pacific Ocean SST decreased the amount of rainfall in the annual time scale (1984-2018). The interaction between rainfall and Pacific Ocean SST was higher in *Kiremt* season than *Belg* and *Bega* seasons. Generally, the occurrence of droughts in the study area was associated with ENSO events like most other parts of Ethiopia and East Africa.

5. Policy Implications

A very good understanding of the distribution, variability, and trend of rainfall and its association with ENSO play an indispensable role in water availability, vegetation distribution, climate change adaptation and mitigation, planning farming practice, and assessment of drought. Hence, the findings of inter-annual variability, trend, and spatial distribution of rainfall in this study should be used to develop a better decision support system in different development activities of West Harerge Zone. Moreover, a good understanding of rainfall is helpful in the hydrological investigation, water resource, and energy development activities. For this reason, the findings of this study should be used as a useful source of information on the spatiotemporal variability and trends of rainfall for climate risk management in and around the drought-prone regions of the study area. Moreover, effective adaptation strategies should be established to combat the adverse impacts of climate change in the study site.

Abbreviations

CHIRPS: Climate Hazards Group Infra-Red Precipitation with Stations; CV: Coefficient of Variation; ENSO: El Niño/Southern Oscillation; MK: Mann-Kendall; MAE: Mean Absolute Error; MBE: Mean Bias Error; NMA: National Meteorological Agency; NOAA: National Oceanic and Atmospheric Administration; NSE: Nash–Sutcliff Efficacy Coefficient; RMSE: Root Mean Square Error; r: Pearson Correlation Coefficient; SST: Sea Surface Temperature; SAI; Standardized Anomaly Index; USGS: United States Geological Survey.

Ethics approval and consent to participate

Not Applicable.

Consent for publication

Not Applicable.

Availability of data and materials

The data for this study can be accessed http://www.cgd.ucar.edu/cas/catalog/climind/TNI_N34/index.html and https://data.chc.ucsb.edu/products/CHIRPS-2.0/ and meteorological rainfall data is accessible in the authors' hand.

Competing Interests

The authors declare that there is no competing of interests.

Funding

The study was fully funded by Oda Bultum University.

Authors' Contributions

All the authors had contributed to data collection and preparation, data analysis, research writing, editing. All authors read and approved the final research manuscript.

Acknowledgments

The authors greatly acknowledge Oda Bultum University and Ethiopian National Meteorological Agency for the financial support and for providing meteorological rainfall data of the study, respectively.

References

Abegaz WB, Mekoya A (2020) Rainfall Variability and Trends over Central Ethiopia. Int J Env Sci Nat Res 24. https://doi.org/10.19080/IJESNR.2020.24.556144

Addisu S, Selassie YG, Fissha G, Gedif B (2015) Time series trend analysis of temperature and rainfall in lake Tana Sub-basin, Ethiopia. Environ Syst Res 4:25. https://doi.org/10.1186/s40068-015-0051-0

Ahmed SI, Rudra R, Dickinson T, Ahmed M (2014)Trend and Periodicity of Temperature Time Series in Ontario. Am J Clim Chang. https://doi.org/10.4236/ajcc.2014.33026

Alemayehu A, Bewket W (2017) Local spatiotemporal variability and trends in rainfall and temperature in the central highlands of Ethiopia. Geogr Ann Ser A Phys Geogr 99: 85–101. https://doi.org/10.1080/04353676.2017.1289460

Alemu MM, Bawoke GT (2019) Analysis of spatial variability and temporal trends of rainfall in the Amhara region, Ethiopia. J Water Clim Chang 1–16. https://doi.org/10.2166/wcc.2019.084

Alhamshry A, Fenta AA, Yasuda H, Kimura R, Shimizu K (2020) Seasonal rainfall variability in Ethiopia and its long-term link to global sea surface temperatures. Water (Switzerland), 12(1). https://doi.org/10.3390/w12010055

Anyah RO, Qiu W (2012) Characteristic 20th and 21st-century precipitation and temperature patterns and changes over the Greater Horn of Africa. Int J Climatol 32: 347–363. https://doi.org/10.1002/joc.2270

Asfaw A, Simane B, Hassen A, Bantider A (2018) Variability and time series trend analysis of rainfall and temperature in north-central Ethiopia: A case study in Woleka sub-basin. Weather Clim Extrem 19: 29–41. https://doi.org/10.1016/j.wace.2017.12.002

Atiah WA, Amekudzi LK, Quansah E, Preko K (2019) The spatiotemporal Variability of Rainfall over the Agro-Ecological Zones of Ghana. Atmos Clim Sci 09: 527–544. https://doi.org/10.4236/acs.2019.93034

Ayalew D, Tesfaye K, Mamo G, Yitaferu B, Bayu W (2012) Variability of rainfall and its current trends in Amhara region, Ethiopia. Afr J Agric Res 7(10):1475–1486

Ayehu GT, Tadesse T, Gessesse B, DinkuT (2018) Validation of new satellite rainfall products over the Upper Blue Nile Basin, Ethiopia. Atmos Meas Tech 11: 1921–1936. https://doi.org/10.5194/amt-11-1921-2018

Babu A (2009) The impact of Pacific sea surface temperature on the Ethiopian rainfall". Workshop on High Impact Weather Predictability Information System for Africa and AMMA THORPEX Forecasters. Trieste, Italy: National Meteorological Agency.

Belay AS, Fenta AA, Yenehun A, Nigate F, Tilahun SA, Moges MM, Dessie M, Adgo E, Nyssen J, Chen M, Van Griensven A, Walraevens K (2019) Evaluation and application of multi-source satellite rainfall product CHIRPS to assess spatiotemporal rainfall variability on data-sparse western margins of Ethiopian highlands. Remote Sens 11:1–22 https://doi.org/10.3390/rs11222688

Birkmann J, Mechler R (2015) Advancing climate adaptation and risk management. New insights, concepts, and approaches: what have we learned from the SREX and the AR5 processes? Climatic Change. https://doi.org/10.1007/s10584-015-1515-y

Bouza-Deaño R, Ternero-Rodríguez M, Fernández-Espinosa AJ (2008) Trend study and assessment of surface water quality in the Ebro River (Spain). J Hydrol 361: 227–239. https://doi.org/10.1016/j.jhydrol.2008.07.048

Camberlin P, Janicot S, Poccard I (2001) Seasonality and atmospheric dynamics of the teleconnection between African rainfall and tropical sea-surface temperature: Atlantic vs. ENSO. *Int J Climatol.* https://doi.org/10.1002/joc.673

Cattani E, Merino A, Guijarro JA, Levizzani V (2018) East Africa Rainfall trends and variability 1983-2015 using three long-term satellite products. Remote Sens .https://doi.org/10.3390/rs10060931

Chen Z, Wen Z, Wu R, Zhao P, Cao J (2014) Influence of two types of El Niños on the East Asian climate during boreal summer: A numerical study. Clim Dyn. https://doi.org/10.1007/s00382-013-1943-1

Cheung WH, Senay GB, Singh A (2008) Trends and spatial distribution of annual and seasonal rainfall in Ethiopia. Int J Climatol 28: 1723–1734. https://doi.org/10.1002/joc.1623

Chou C, Lan CW (2012) Changes in the annual range of precipitation under global warming. J Clim. https://doi.org/10.1175/JCLI-D-11-00097.1

Conway D, Schipper ELF (2011) Adaptation to climate change in Africa: Challenges and opportunities identified from Ethiopia. GlobEnviron Chang 21: 227–237. https://doi.org/10.1016/j.gloenvcha.2010.07.013

Dawit M, Halefom A, Teshome A, Sisay E, Shewayirga B, Dananto M (2019) Changes and variability of precipitation and temperature in the Guna Tana watershed, Upper Blue Nile Basin, Ethiopia. Model Earth Syst Environ 0123456789. https://doi.org/10.1007/s40808-019-00598-8

De Luís M, Raventós J, González-Hidalgo JC, Sánchez JR, Cortina J (2000) Spatial analysis of rainfall trends in the region of valencia (East Spain). International Journal of Climatology 20: 1451–1469.

Degefu MA, Bewket W (2014) Variability and trends in rainfall amount and extreme event indices in the Omo-Ghibe River Basin, Ethiopia. Reg Environ Chang 14: 799–810. https://doi.org/10.1007/s10113-013-0538-z

Degefu MA, Rowell DP, Bewket W (2017) Teleconnections between Ethiopian rainfall variability and global SSTs: observations and methods for model evaluation. Meteorol Atmos Phys 129: 173–186. https://doi.org/10.1007/s00703-016-0466-9

Dinku T, Ceccato P, Grover-Kopec E, Lemma M, Connor SJ, Ropelewski CF (2007) Validation of satellite rainfall products over East Africa's complex topography. Int J Remote Sens 28: 1503–1526. https://doi.org/10.1080/01431160600954688

Dinku T, Funk C, Peterson P, Maidment R, Tadesse T, Gadain H, Ceccato P (2018) Validation of the CHIRPS satellite rainfall estimates over eastern Africa. Q J R Meteorol Soc 144: 292–312. https://doi.org/10.1002/qj.3244

Dinku T, Hailemariam K, Maidment R, Tarnavsky E, Connor S (2014) The combined use of satellite estimates and rain gauge observations to generate high-quality historical rainfall time series over Ethiopia. Int J Climatol 34: 2489–2504.https://doi.org/10.1002/joc.3855
Diro GT, Grimes DIF, Black E (2011) Teleconnections between Ethiopian summer rainfall and sea surface temperature: Part I-observation and modeling. Clim Dyn 37: 103–119. https://doi.org/10.1007/s00382-010-0837-8
Elliott J, Deryng D, Müller C, Frieler K, Konzmann M, Gerten D, Glotter M, Flörke M, Wada Y, Best N, Eisner S, Fekete BM, Folberth C, Foster I, Gosling SN, Haddeland I, Khabarov N, Ludwig F, Masaki Y, … Wisser D (2014) Constraints and potentials of future irrigation water availability on agricultural production under climate change. Proc Natl Acad Sci USA. https://doi.org/10.1073/pnas.1222474110
FAO (2019) 2018/19 El Niño High-risk countries and potential impacts on food security and agriculture.
Fekadu K (2015) Ethiopian Seasonal Rainfall Variability and Prediction Using Canonical Correlation Analysis (CCA). Earth Sciences 4: 112. https://doi.org/10.11648/j.earth.20150403.14
Feng G, Cobb S, Abdo Z., Fisher DK, Ouyang Y, Adeli A, Jenkins JN (2016)Trend analysis and forecast of precipitation, reference evapotranspiration, and rainfall deficit in the blackland prairie of eastern Mississippi. J Appl Meteorol Climatol. https://doi.org/10.1175/JAMC-D-15-0265.1
Fenta AA, Yasuda H, Shimizu K, Ibaraki Y, Haregeweyn N, Kawai T, Belay AS, Sultan D, Ebabu K (2018) Evaluation of satellite rainfall estimates over the Lake Tana basin at the source region of the Blue Nile River. Atmos Res 212: 43–53. https://doi.org/10.1016/j.atmosres.2018.05.009
Funk C, Peterson P, Landsfeld M, Pedreros D, Verdin J, Shukla S, Husak G, Rowland J, Harrison L, Hoell A, Michaelsen J (2015) The climate hazards infrared precipitation with stations - A new environmental record for monitoring extremes. Sci Data 2. https://doi.org/10.1038/sdata.2015.66
Ganguly AR, Kumar D, Ganguli P, Short G, Klausner J (2015) Climate Adaptation Informatics: Water Stress on Power Production. Comput Sci Eng.https://doi.org/10.1109/MCSE.2015.106
Gebrechorkos SH, Hülsmann S, Bernhofer C (2019) Long-term trends in rainfall and temperature using high-resolution climate datasets in East Africa. Scientific Reports 9:11376. https://doi.org/10.1038/s41598-019-47933-8
Gebrehiwot T, VanDerVeen V (2013) Assessing the evidence of climate variability in the northern Ethiopia. J Dev Agric Econ 5: 104–119
Gebremichael M, Krajewski WF, Morrissey ML, Huffman GJ, Adler RF (2005) A detailed evaluation of GPCP 1° daily rainfall estimates over the Mississippi River basin. J Appl Meteorol 44: 665–681. https://doi.org/10.1175/JAM2233.1
Gedefaw M, Yan D, Wang H, Qin T, Girma A, Abiyu A, Batsuren D (2018) Innovative trend analysis of annual and seasonal rainfall variability in Amhara Regional State, Ethiopia. Atmosphere (Basel) 9. https://doi.org/10.3390/atmos9090326
Gemechu D (1988) Some Patterns of Altitudinal Variation of Climatic Elements in the Mountainous Regions of Ethiopia. Mt Res Dev 8: 131–138
Geremew GM, Mini S, Abegaz A (2020) Spatiotemporal variability and trends in rainfall extremes in Enebsie Sar Midir district, northwest Ethiopia. Model Earth Syst Environ 6: 1177–1187. https://doi.org/10.1007/s40808-020-00749-2
Gissila T, Black E, Grimes DIF, Slingo JM (2004) Seasonal forecasting of the Ethiopian summer rains. Int J Climatol 24: 1345–1358. https://doi.org/10.1002/joc.1078
Gocic M, Trajkovic S (2013) Analysis of changes in meteorological variables using Mann-Kendall and Sen's slope estimator statistical tests in Serbia. Glob Planet Change 100: 172–182. https://doi.org/10.1016/j.gloplacha.2012.10.014
Goshime DW, Absi R, Ledésert B (2019) Evaluation and Bias Correction of CHIRP Rainfall Estimate for Rainfall-Runoff Simulation over Lake Ziway Watershed, Ethiopia. Hydrology 6: 1–22. https://doi:10.3390/hydrology6030068
Gummadi S, Rao KPC, Seid J, Legesse G, Kadiyala MDM, Takele R, Amede T, Whitbread A (2018) Spatio-temporal variability and trends of precipitation and extreme rainfall events in Ethiopia in 1980–2010.Theor Appl Climatol. https://doi.org/10.1007/s00704-017-2340-1
Guo W, Ni X, Jing D, Li S (2014) Spatial-temporal patterns of vegetation dynamics and their relationships to climate variations in Qinghai Lake Basin using MODIS time-series data. J Geogr Sci 24: 1009–1021. https://doi.org/10.1007/s11442-014-1134-y
Hamlaoui-Moulai L, Mesbah M, Souag-Gamane D, Medjerab A (2013) Detecting hydro-climatic change using spatiotemporal analysis of rainfall time series in Western Algeria. Nat Hazards 65: 1293–1311. https://doi.org/10.1007/s11069-012-0411-2
Hao Z, Aghakouchak A (2014) A nonparametric multivariate multi-index drought monitoring framework. J Hydrometeorol 15: 89–101. https://doi.org/10.1175/JHM-D-12-0160.1
IPCC (Intergovernmental Panel on Climate Change) (2007) Climate Change 2007 - The Physical Science Basis

Contribution of Working Group I to the Fourth Assessment Report of the IPCC, Cambridge University Press, Cambridge, UK
IPCC (2012) Managing the Risks of Extreme Events and Disasters to Advance Climate Change Adaptation: A Special Report of Working Groups I and II of the Intergovernmental Panel on Climate Change [Field, C.B., V. Barros, T.F. Stocker, D. Qin, D.J. Dokken, K.L. Ebi, M.D. Mastrandrea, K.J. Mach, G.-K. Plattner, S.K. Allen, M. Tignor, and P.M. Midgley (eds.)]. Cambridge University Press, Cambridge, UK, and New York, NY, USA, 582 pp
IPCC (2014) Climate Change 2014: Mitigation of Climate Change. Summary for Policymakers and Technical Summary. In Climate Change 2014: Mitigation of Climate Change. Part of the Working Group III Contribution to the Fifth Assessment Report of the IPCC, Geneva, Switzerland. https://doi.org/10.1017/CBO9781107415416.005
IPCC (2018) Climate change 2018: impact of 1.5°C global warming on natural and human systems [Masson-Delmottee V, Zhai P, Portner H-O, Roberts D, Skea J, Shukla PR, Pirani A, Moufouma-Okia W, Peans C, Pidcock R, Connors S, Matthews JBR, Chen Y, Zhou X, Gomis MI, Lonnoy E, Maycock T, Tignor M, Waterfeld T (eds)] (in press)
Jain SK, Kumar V (2012) Trend analysis of rainfall and temperature data for India. Current Science.
Jajcay N, Kravtsov S, Sugihara G, Tsonis AA, Paluš M (2018) Synchronization and causality across time scales in El Niño Southern Oscillation. npj Clim Atmos Sci 1.https://doi.org/10.1038/s41612-018-0043-7
Jury MR, Funk C (2013) Climatic trends over Ethiopia: Regional signals and drivers. Int J Climatol 33: 1924–1935. https://doi.org/10.1002/joc.3560
Kassie BT, Hengsdijik H, Rotter RP, Kahiluoto H, Asseng S, VanIttersum MK (2013) Adapting to climate variability and change: experiences from cereal based farming in the central rift and Kobo Valleys, Ethiopia. Environ Manag 52:1115–1131
Katsanos D, Retalis A, Michaelides S (2016) Validation of a high-resolution precipitation database (CHIRPS) over Cyprus for a 30-year period. Atmos Res 169: 459–464. https://doi.org/10.1016/j.atmosres.2015.05.015
Kendall MG (1975) Rank Correlation Methods. The Statistician 20. https://doi.org/10.2307/2986801
Kimani MW, Hoedjes JCB, Su Z (2017) An assessment of satellite-derived rainfall products relative to ground observations over East Africa. Remote Sens 9. https://doi.org/10.3390/rs9050430
Knapp KR, Ansari S, Bain CL, Bourassa MA, Dickinson MJ, Funk C, Helms CN, Hennon CC, Holmes CD, Huffman GJ, Kossin JP, Lee HT, Loew A, Magnusdottir G (2011) Globally Gridded Satellite observations for climate studies. Bull Am Meteorol Soc 92: 893–907. https://doi.org/10.1175/2011BAMS3039.1
Korecha D, Barnston AG (2007) Predictability of June-September rainfall in Ethiopia. Mon Weather Rev 135: 628–650. https://doi.org/10.1175/MWR3304.1
Larbi I, Hountondji FCC, Annor T, Agyare WA, Gathenya JM, Amuzu J (2018) Spatiotemporal trend analysis of rainfall and temperature extremes in the Vea catchment, Ghana. Climate 6: 1–17. https://doi.org/10.3390/cli6040087
Li C, Qi J, Yang L, Wang S, Yang W, Zhu G, Zou S, Zhang F (2014) Regional vegetation dynamics and its response to climate change - A case study in the Tao River Basin in Northwestern China. Environ Res Lett 9.https://doi.org/10.1088/1748-9326/9/12/125003
Loua RT, Bencherif H, Mbatha N, Bègue N, Hauchecorne A, Bamba Z, Sivakumar V (2019) Study on Temporal Variations of Surface Temperature and Rainfall at Conakry Airport, Guinea: 1960–2016. Climate 7: 93. https://doi.org/10.3390/cli7070093
Lyon B (2014) Seasonal drought in the Greater Horn of Africa and its recent increase during the March-May long rains. J Clim. https://doi.org/10.1175/JCLI-D-13-00459.1
Mann HB (1945) Nonparametric Tests Against Trend. Econometrica 13: 245. https://doi.org/10.2307/1907187
McKee TB, Nolan J, Kleist J (1993) The relationship of drought frequency and duration to time scales. Preprints, Eighth Conf. on Applied Climatology. Amer Meteor Soc.
Mekasha A, Tesfaye K, Duncan AJ (2014)Trends in daily observed temperature and precipitation extremes over three Ethiopian eco-environments. Int J Climatol. https://doi.org/10.1002/joc.3816
Mekonen AA, Berlie AB, Ferede MB (2020) Spatial and temporal drought incidence analysis in the northeastern highlands. Geoenvironmental Disasters 7.
Mengistu D, Bewket W, Lal R (2014)Recent spatiotemporal temperature and rainfall variability and trends over the Upper Blue Nile River Basin, Ethiopia. Int J Climatol 34: 2278–2292. https://doi.org/10.1002/joc.3837
Meze-Hausken E (2004) Contrasting climate variability and meteorological drought with perceived drought and climate change in northern Ethiopia. Clim Res 27: 19–31. https://doi.org/10.3354/cr027019
Mitchell JM, Dzerdzeevskii B, Flohn H, Hofmeyr WL, Lamb HH, Rao KN, Wallén CC (1966) Climatic change. WMO Technical Note, 79 (WMO-No. 195/TP. 100). World Meteorological Organization, Geneva
MOA (2000) Agro-ecological zones of Ethiopia. Ministry of Agriculture (MOA), Addis Ababa, Ethiopia. Bulletin Fuer Angewandte Geologie. https://doi.org/10.5169/seals-391142

Mohammed Y, Yimer F, Tadesse M, Tesfaye K (2018) Variability and trends of rainfall extreme events in the northeast highlands of Ethiopia. Int J Hydrol 2: 594–605. https://doi.org/10.15406/ijh.2018.02.00131
Moloro TL (2018) Spatio-temporal Analysis of Rainfall Variability and Meteorological Drought : A Case Study in Bilate River Basin, Southern Rift Valley, Ethiopia. Int J Env Sci Nat Res 14. https://doi.org/10.19080/IJESNR.2018.14.555891
Mu S, Yang H, Li J, Chen Y, Gang C, Zhou W, Ju W (2013) Spatio-temporal dynamics of vegetation coverage and its relationship with climate factors in Inner Mongolia, China. J Geogr Sci 23: 231–246. https://doi.org/10.1007/s11442-013-1006-x
Mulugeta S, Fedler C, Ayana M (2019) Analysis of long-term trends of annual and seasonal rainfall in the Awash River Basin, Ethiopia. Water (Switzerland) 11. https://doi.org/10.3390/w11071498
Muthoni FK, Odongo VO, Ochieng J, Mugalavai EM, Mourice SK, Hoesche-Zeledon I, Mwila M, Bekunda M (2019) Long-term spatial-temporal trends and variability of rainfall over Eastern and Southern Africa. Theor Appl Climatol 137: 1869–1882. https://doi.org/10.1007/s00704-018-2712-1
Nash J E, Sutcliffe JV (1970) River flow forecasting through conceptual models part I - A discussion of principles. J Hydrol 10: 282–290. https://doi.org/10.1016/0022-1694(70)90255-6
Omondi PAo, Awange JL, Forootan E, Ogallo LA, Barakiza R, Girmaw GB, Fesseha I, Kululetera V, Kilembe C, Mbati MM, Kilavi M, King'uyu SM, Omeny PA, Njogu A, Badr EM, Musa TA, Muchiri P, Bamanya D, Komutunga E (2014) Changes in temperature and precipitation extremes over the Greater Horn of Africa region from 1961 to 2010. Int J Climatol. https://doi.org/10.1002/joc.3763
OWWDSE (2010) East Hararge and West Hararge Zone Land Use Plan Study Project: Arba Kurkura Sub Basin Integrated Land Use. Oromia Water Works Design and Supervision (OWWDSE), Addis Ababa, Ethiopia.30 pp. October, Cd.
Pal AB, Khare D, Mishra PK, Singh L (2017) Trend Analysis of Rainfall, Temperature, and Runoff Data: a Case Study of Rangoon Watershed in Nepal. Int J Students' Res Technol Manag 5: 21–38. https://doi.org/10.18510/ijsrtm.2017.535
Panthi J, Dahal P, Shrestha ML, Aryal S, Krakauer NY, Pradhanang SM, Lakhankar T, Jha AK, Sharma M, Karki R (2015) Spatial and temporal variability of rainfall in the Gandaki River Basin of Nepal Himalaya. Climate 3: 210–226. https://doi.org/10.3390/cli3010210
Pegion K, Kirtman BP (2008) The impact of air-sea interactions on the simulation of tropical intraseasonal variability. J Clim 21: 6616–6635. https://doi.org/10.1175/2008JCLI2180.1
Philip SJ (2018) Effects of Climate Change on Sea Levels and Inundation Relevant to the Pacific Islands. Science Review 43–49
Poudel S, Shaw R (2016) The relationships between climate variability and crop yield in a mountainous environment: A case study in Lamjung District, Nepal. Climate. https://doi.org/10.3390/cli4010013
Qian X, Liang L, Shen Q, Sun Q, Zhang L, Liu Z, Zhao S, Qin Z (2016) Drought trends based on the VCI and its correlation with climate factors in the agricultural areas of China from 1982 to 2010. Environ Monit Assess 188. https://doi.org/10.1007/s10661-016-5657-9
Ratnam JV, Behera SK, MasumotoY, Yamagata T (2014) Remote effects of El Niño and Modoki events on the austral summer precipitation of Southern Africa. J Clim 27: 3802–3815. https://doi.org/10.1175/JCLI-D-13-00431.1
Saeidizand R, Sabetghadam S, Tarnavsky E, Pierleoni A (2018) Evaluation of CHIRPS rainfall estimates over Iran. Q J R Meteorol Soc 144: 282–291. https://doi.org/10.1002/qj.3342
Segele ZT, Lamb PJ (2005) Characterization and variability of *Kiremt* rainy season over Ethiopia. Meteorol Atmos Phys 89: 153–180. https://doi.org/10.1007/s00703-005-0127-x
Seleshi Y, Camberlin P (2006) Recent changes in a dry spell and extreme rainfall events in Ethiopia. Theor Appl Climatol 83: 181–191. https://doi.org/10.1007/s00704-005-0134-3
Sen PK (1968) Estimates of the Regression Coefficient Based on Kendall's Tau. J Am Stat Assoc 63: 1379–1389. https://doi.org/10.1080/01621459.1968.10480934
Seneshaw G, Yitea S (2015) Analysis of Climate Variability (ENSO) and Vegetation Dynamics in Gojjam, Ethiopia. J Earth Sci Clim Change 06. https://doi.org/10.4172/2157-7617.1000320
Shanko D, Camberlin P (1998) The effects of the southwest Indian ocean tropical cyclones on Ethiopian drought. Int J Climatol 18: 1373–1388.
Suryabhagavan KV (2017) GIS-based climate variability and drought characterization in Ethiopia over three decades. Weather Clim Extrem 15: 11–23. https://doi.org/10.1016/j.wace.2016.11.005
Taye MT, Zewdu F (2012) Spatio-temporal variability and trend of rainfall and temperature in western Amhara, Ethiopa: a GIS approach. Global advanced research. J Geogr Reg Plan 1(4):65–82
Tesfamariam BG. Gessesse B, Melgani F(2019) Characterizing the spatiotemporal distribution of meteorological drought as a response to climate variability : The case of rift valley lakes basin of Ethiopia. Weather Clim Extrem 26: 100237. https://doi.org/10.1016/j.wace.2019.100237
Tierney JE, Smerdon JE, Anchukaitis KJ, Seager R (2013) Multidecadal variability in East African

hydroclimate controlled by the Indian Ocean. Nature. https://doi.org/10.1038/nature11785
Tierney JE, Ummenhofer CC, DeMenocal PB (2015) Past and future rainfall in the Horn of Africa. Sci Adv1. https://doi.org/10.1126/sciadv.1500682
Tiruneh GB, Gessesse B, Besha T, Workineh G (2018) Evaluating the Association between Climate Variability and Vegetation Dynamics by Using Remote Sensing Techniques : The Case of Upper Awash Basin, Ethiopia. World J Agric Res 6: 153–166. https://doi.org/10.12691/wjar-6-4-6
Toté C, Patricio D, Boogaard H, van der Wijngaart R, Tarnavsky E, Funk C (2015) Evaluation of satellite rainfall estimates for drought and flood monitoring in Mozambique. Remote Sens 7: 1758–1776. https://doi.org/10.3390/rs70201758
Traore SS, Landmann T, Forkuo EK, Traore PCS (2014) Assessing Long-Term Trends In Vegetation Productivity Change Over the Bani River Basin in Mali (West Africa). J Geogr Earth Sci 2. https://doi.org/10.15640/jges.v2n2a2
Viste E, Korecha D, Sorteberg A (2013) Recent drought and precipitation tendencies in Ethiopia. Theor Appl Climatol 112: 535–551. https://doi.org/10.1007/s00704-012-0746-3
Viste E, Sorteberg A (2013) Moisture transport into the Ethiopian highlands. Int J Climatol. https://doi.org/10.1002/joc.3409
Wagesho N, Goel NK, Jain MK (2013) Temporal and spatial variability of annual and seasonal rainfall over Ethiopia. Hydrol Sci J 58: 354–373. https://doi.org/10.1080/02626667.2012.754543
Wang Y, You W, Fan J, Jin M, Wei X, Wang Q (2018) Effects of subsequent rainfall events with different intensities on runoff and erosion in a coarse soil. Catena. https://doi.org/10.1016/j.catena.2018.06.008
Weldegerima TM, Zeleke TT, Birhanu BS, Zaitchik BF, Fetene ZA (2018) Analysis of Rainfall Trends and Its Relationship with SST Signals in the Lake Tana Basin, Ethiopia. Adv Meteorol 2018. https://doi.org/10.1155/2018/5869010
Wondosen N (2017) Agricultural drought risk area assessment and mapping using Remote Sensing and GIS: a case study of west Hararge Zone, Ethiopia. Addis Ababa University.
Worku LY (2015) Climate change impact on variability of rainfall intensity in the Upper Blue Nile Basin. IAHS-AISH Proceedings and Reports. https://doi.org/10.5194/piahs-366-135-2015
Worku T, Khare D, Tripathi S K (2019) Spatiotemporal trend analysis of rainfall and temperature, and its implications for crop production. J Water Clim Chang. https://doi.org/10.2166/wcc.2018.064
Wu R, Kirtman BP, Pegion K (2008) Local rainfall-SST relationship on subseasonal time scales in satellite observations and CFS. Geophys Res Lett. https://doi.org/10.1029/2008GL035883
Yasuda H, Panda SN, Abd Elbasit MAM, Kawai T, Elgamri T, Fenta AA, Nawata H (2018) Teleconnection of rainfall time series in the central Nile Basin with sea surface temperature. Paddy Water Environ 16: 805–821. https://doi.org/10.1007/s10333-018-0671-x
Yin Z, Dong Q, Kong F, Cao D, Long S (2020) Seasonal and interannual variability of the Indo-Pacific Warm Pool and its associated climate factors based on remote sensing. Remote Sens 12. https://doi.org/10.3390/rs12071062
Yu B, Zhang X, Lin H, Yu JY (2015) Comparison of Wintertime North American Climate Impacts Associated with Multiple ENSO Indices. Atmos Ocean. https://doi.org/10.1080/07055900.2015.1079697
Yue S, Pilon P, Cavadias G (2002) Power of the Mann-Kendall and Spearman's rho tests for detecting monotonic trends in hydrological series. J Hydrol 259: 254–271. https://doi.org/10.1016/S0022-1694(01)00594-7
Zaroug M (2010) The connections of Pacific SST and drought over East Africa". DEWFORA meeting at ECMWF, Improved Drought Early Warning and Forcasting to strengthen preparedness and adaptation to droughts in Africa (DEWFORA). United Kingdom 4-5 October.
Zhang Q, Singh VP, Li J, Chen X (2011) Analysis of the periods of maximum consecutive wet days in China. J Geophys Res Atmos. https://doi.org/10.1029/2011JD016088
Zhang Q, Xu CY, Zhang Z, Chen YD (2010) Changes of atmospheric water vapor budget in the Pearl River basin and possible implications for hydrological cycle. Theor Appl Climatol. https://doi.org/10.1007/s00704-010-0257-z
Zhao W, Yu X, Ma H, Zhu Q, Zhang Y, Qin W, Ai N, Wang Y (2015) Analysis of precipitation characteristics during 1957-2012 in the semi-arid loess Plateau, China. PLoS ONE. https://doi.org/10.1371/journal.pone.0141662

Figures

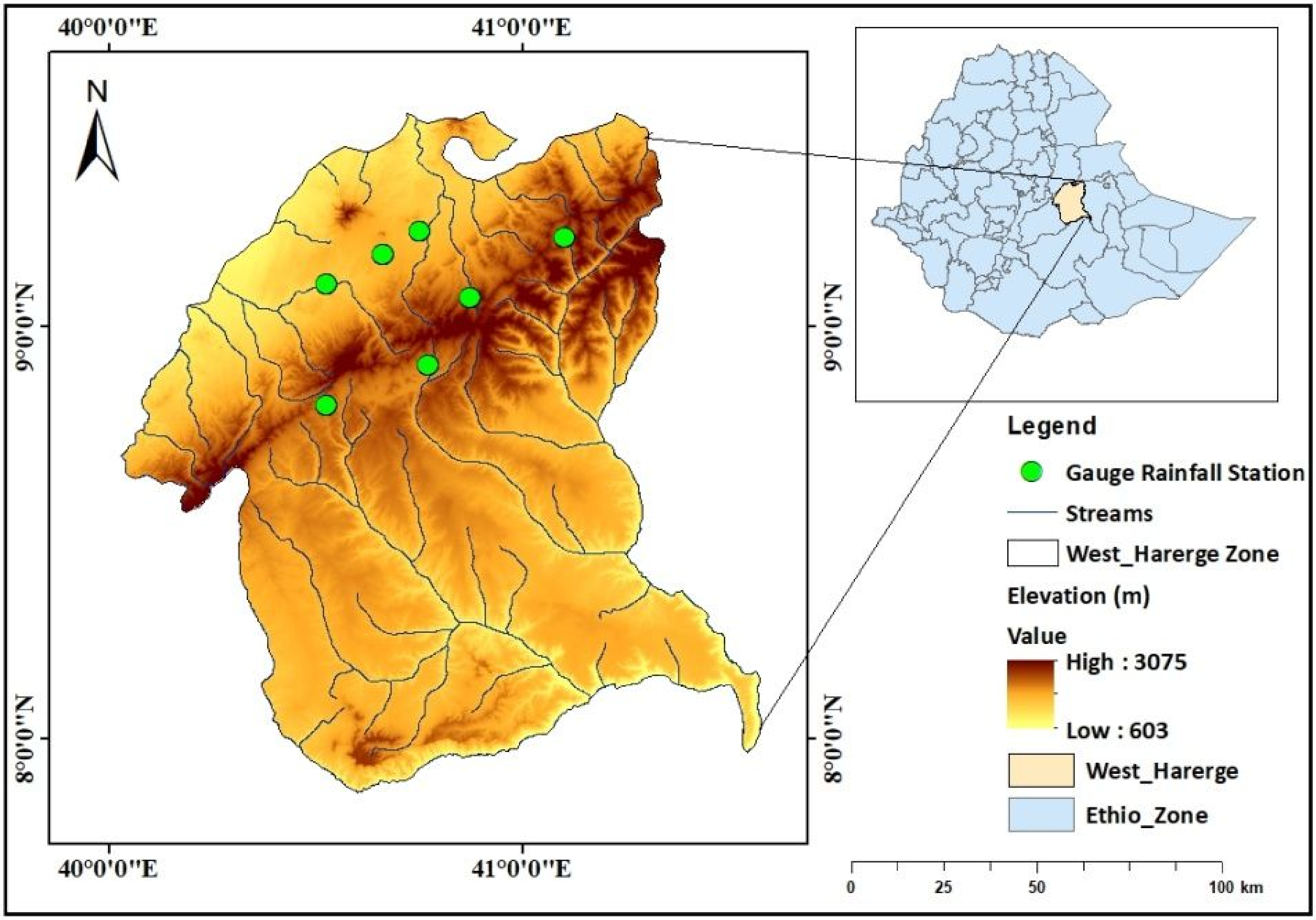

Figure 1

Location map of the study area

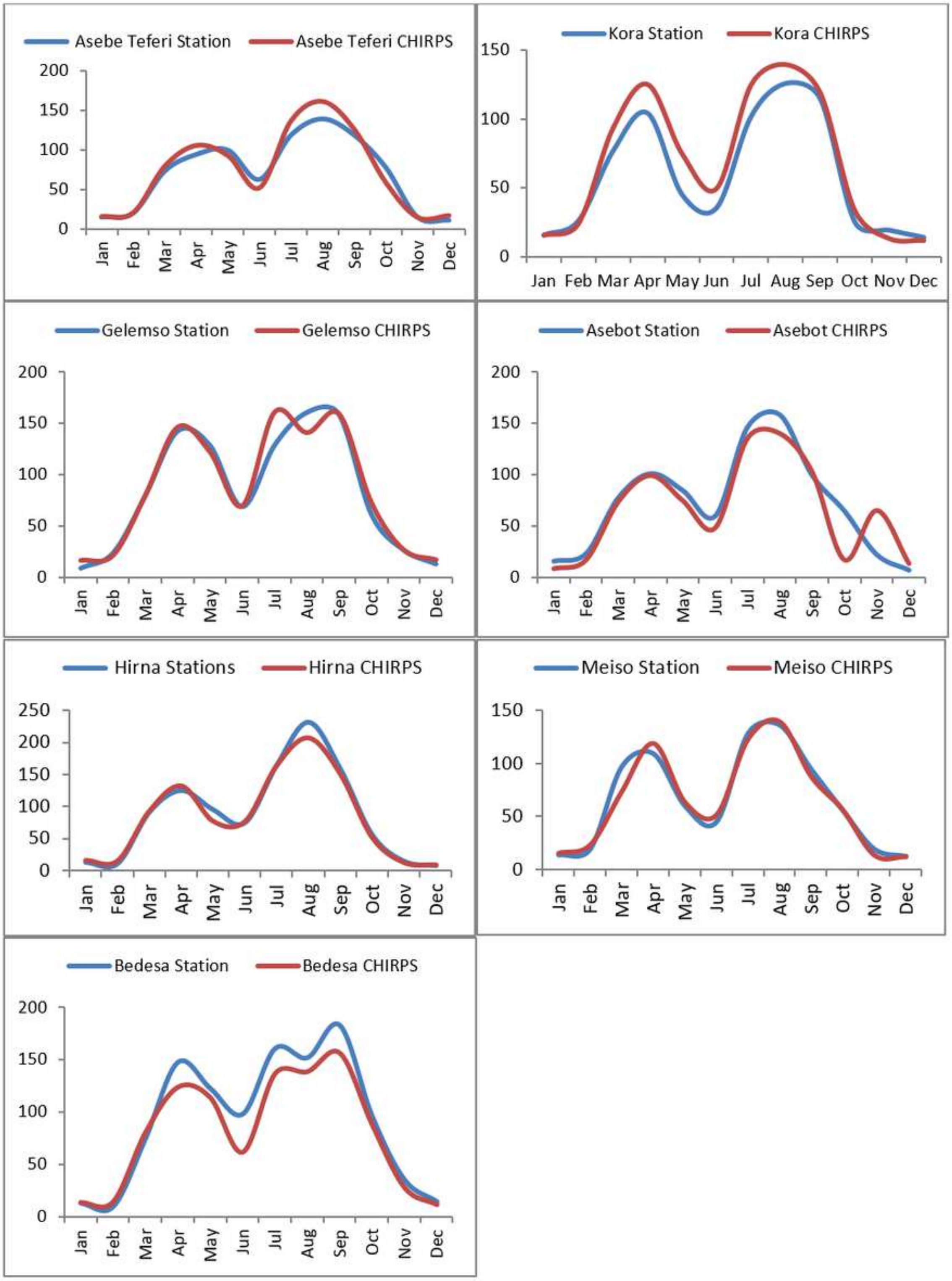

Figure 2

Graphical comparison of mean monthly CHIRPS and meteorological station rainfall in the West Harerge Zone

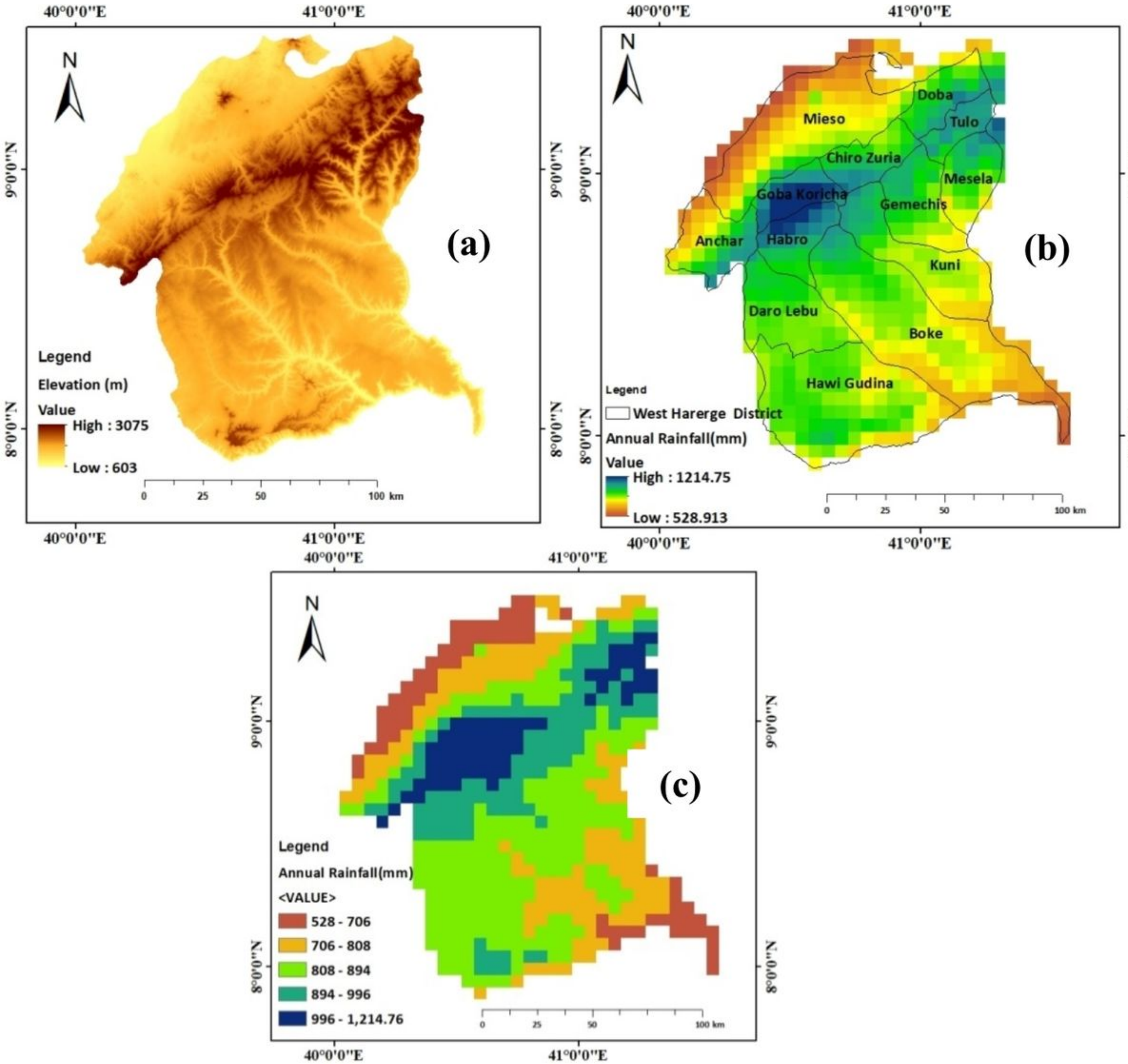

Figure 3

Elevation (a), spatial distributions of long-term mean annual rainfall (mm) across the district (b) and spatial distributions of long-term mean annual rainfall (c) of West Harerge Zone (1983-2019)

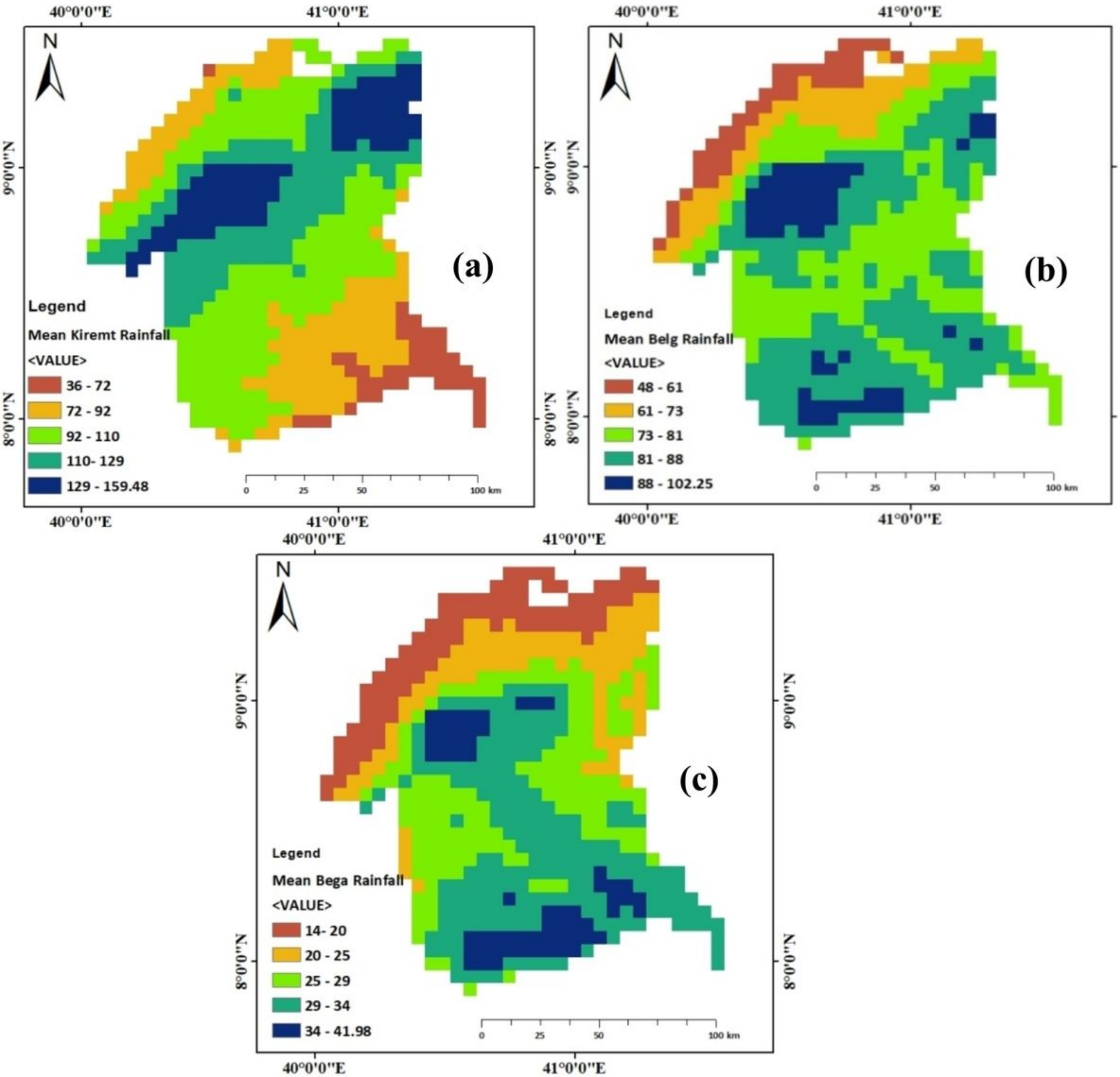

Figure 4

Spatial distributions of mean average Kiremt rainfall (mm) (a) mean average Belg rainfall (mm) (b) and mean average Bega rainfall (mm) (c) of the West Harerge Zone (1983-2019)

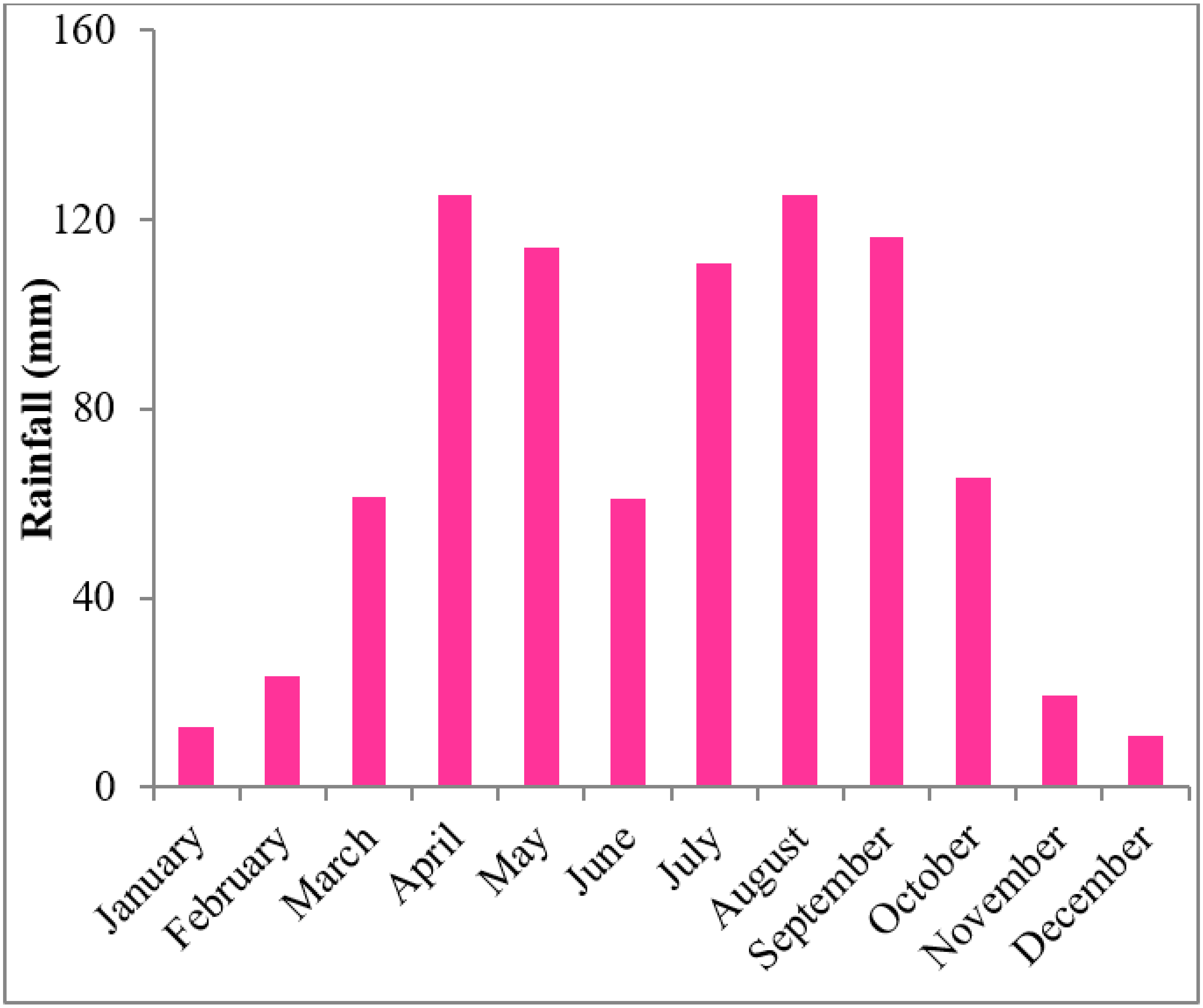

Figure 5

Mean monthly rainfall of West Harerge Zone during 1983-2019 periods

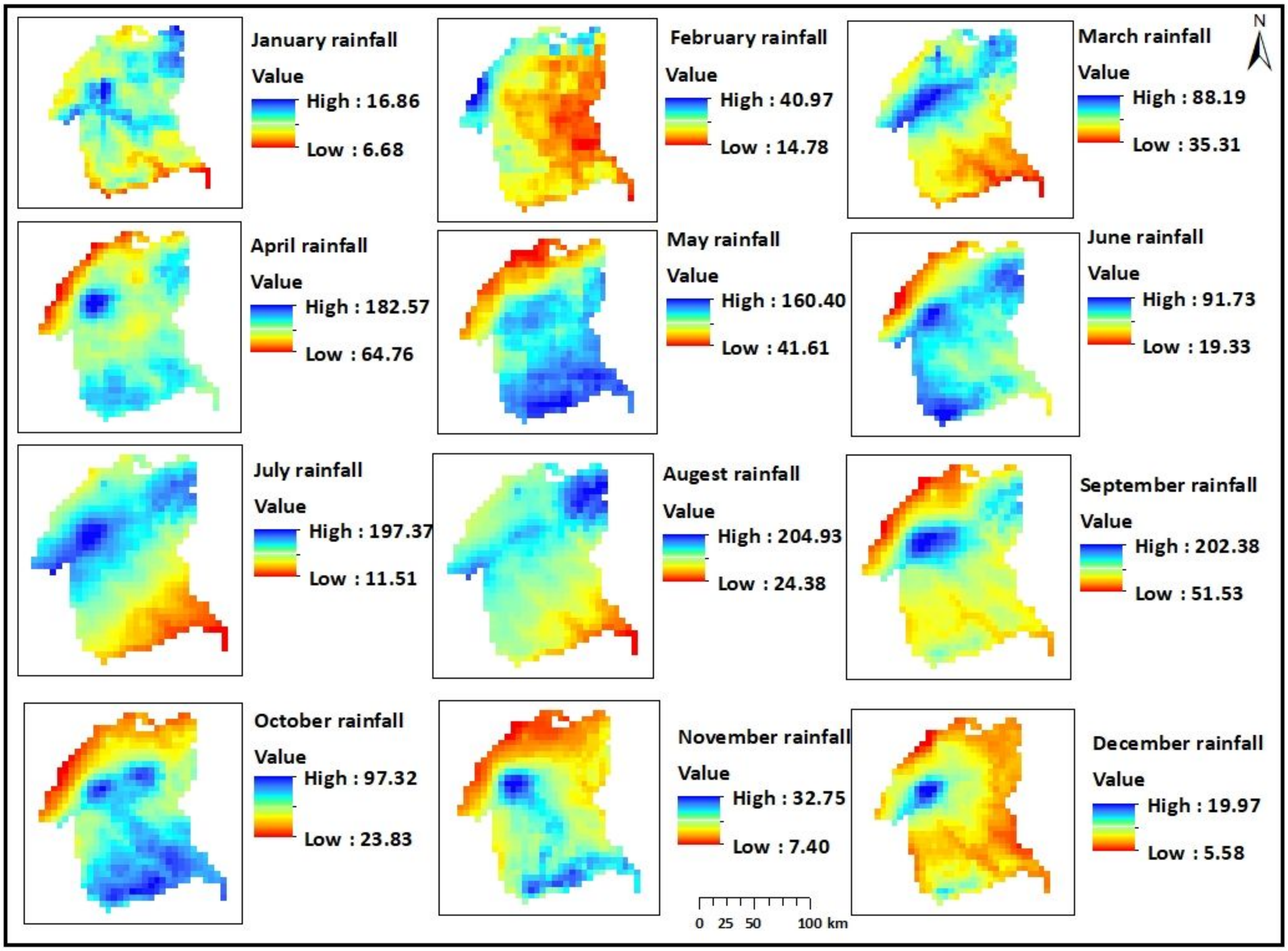

Figure 6

Spatial distributions of mean monthly rainfall of West Harerge Zone (1983-2019)

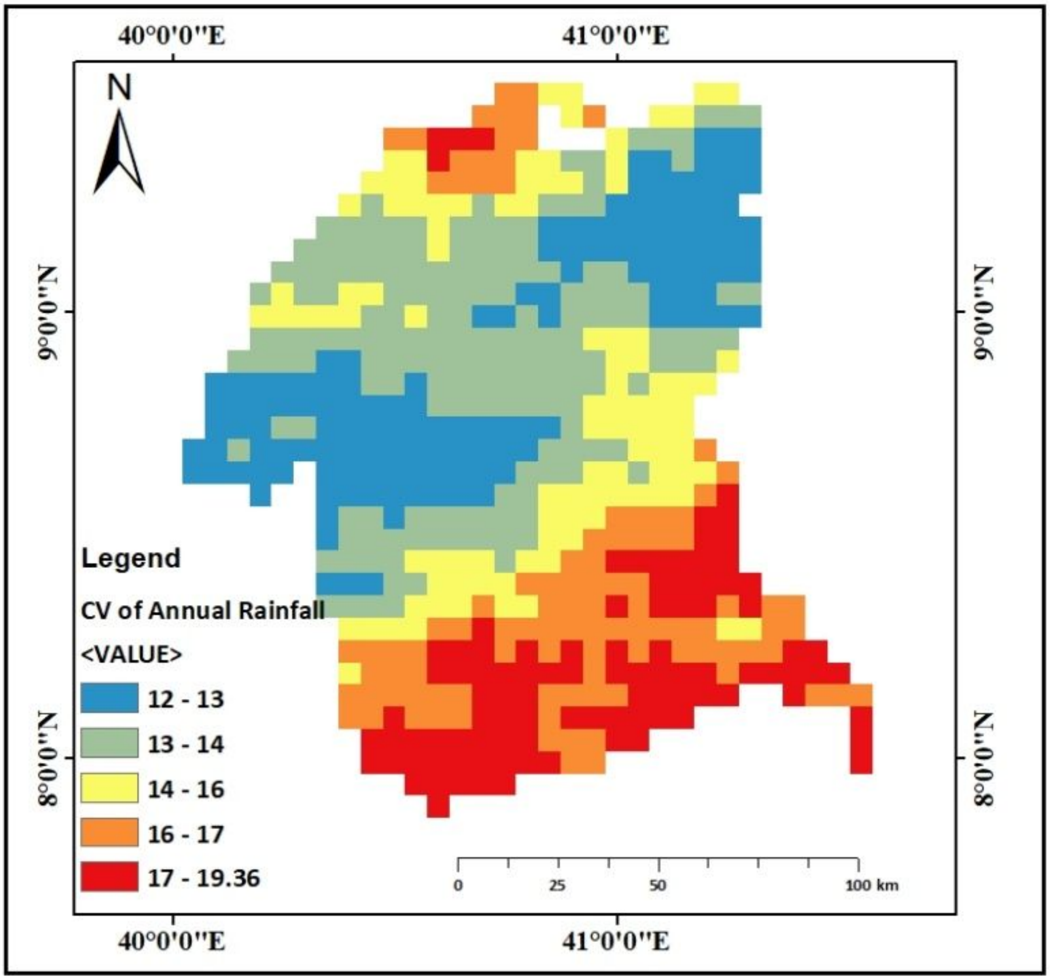

Figure 7

Spatial distribution of CV (%) of annual rainfall in West Harerge Zone (1983-2019)

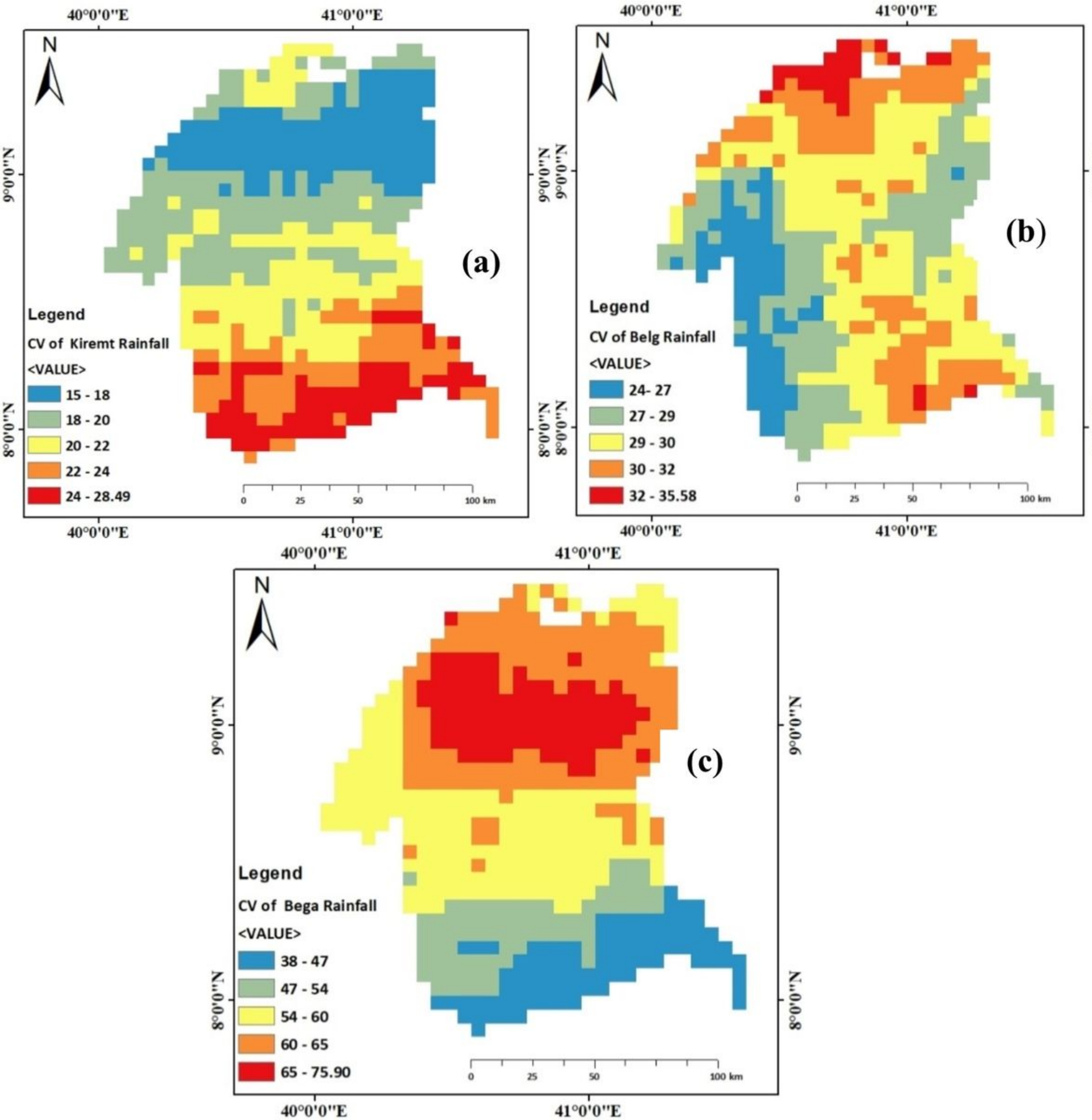

Figure 8

Spatial distribution of CV (%) in Kiremt (a), Belg (b), and Bega (c) season rainfall in West Harerge Zone (1983-2019)

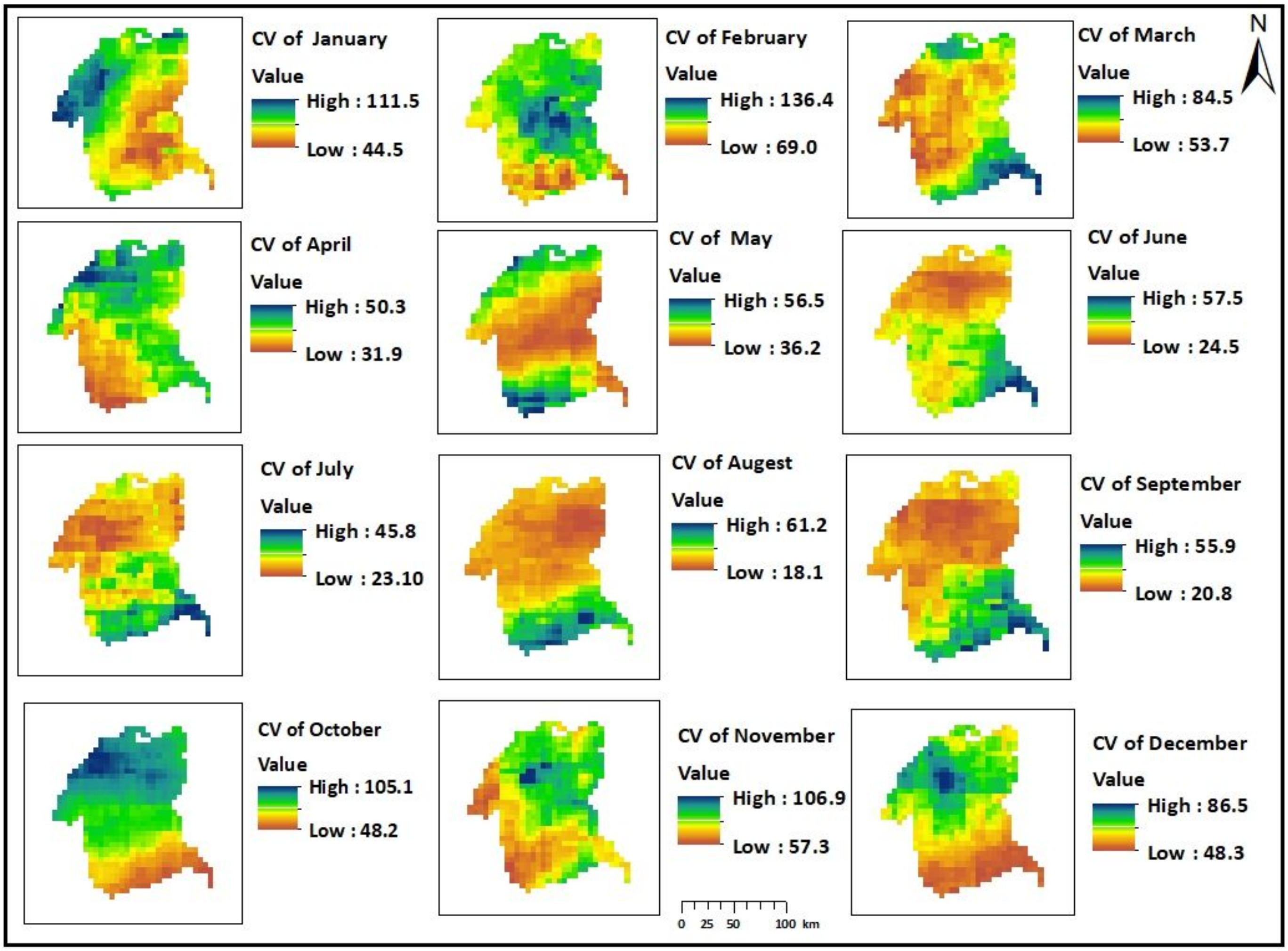

Figure 9

Spatial distribution of monthly rainfall CV (%) of West Harerge Zone (1983-2019)

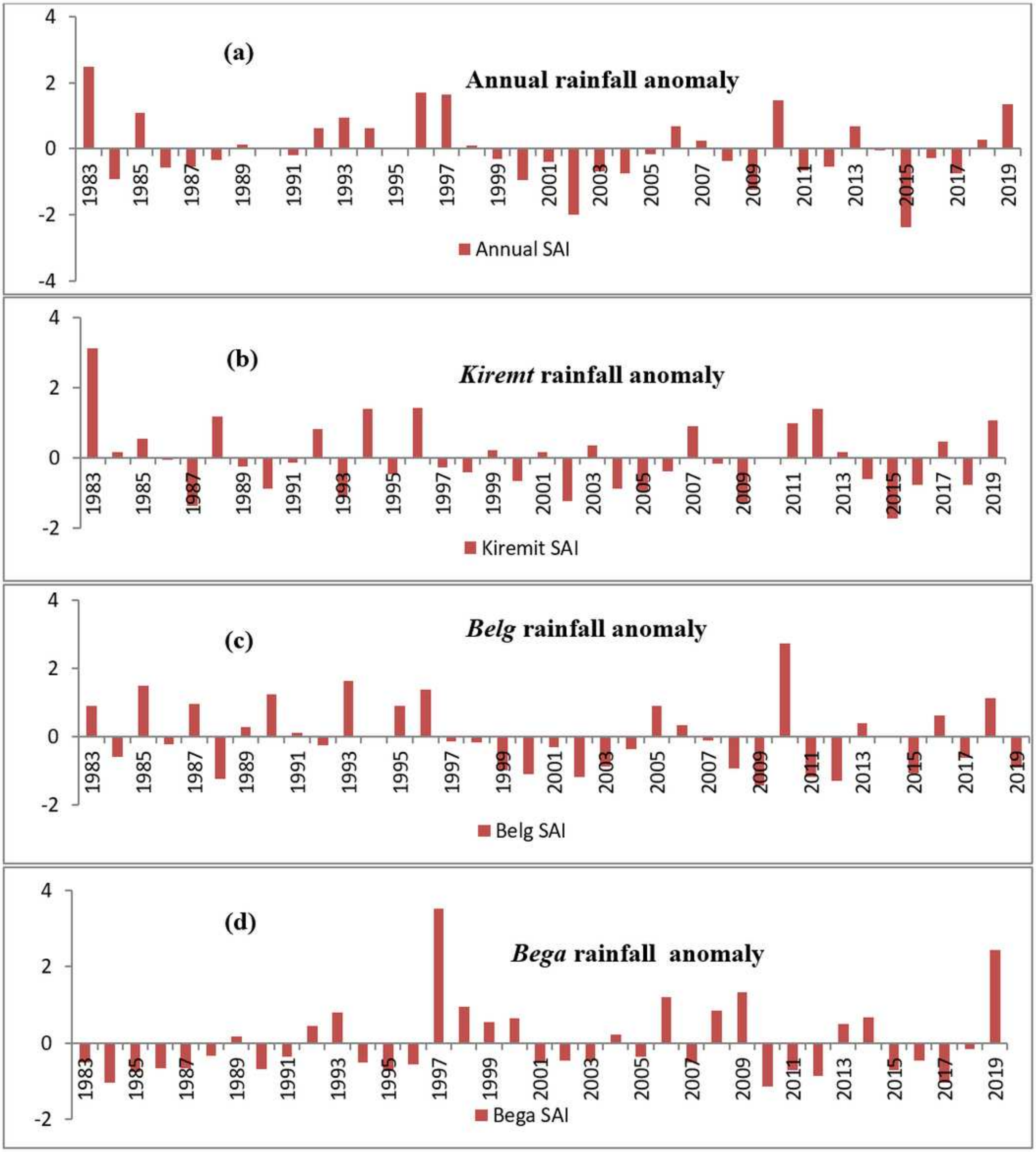

Figure 10

Annual rainfall SAI (a), mean Kiremt rainfall SAI (b), mean Belg rainfall SAI (c), and mean Bega rainfall SAI (d) of West Harerge Zone (1983-2019)

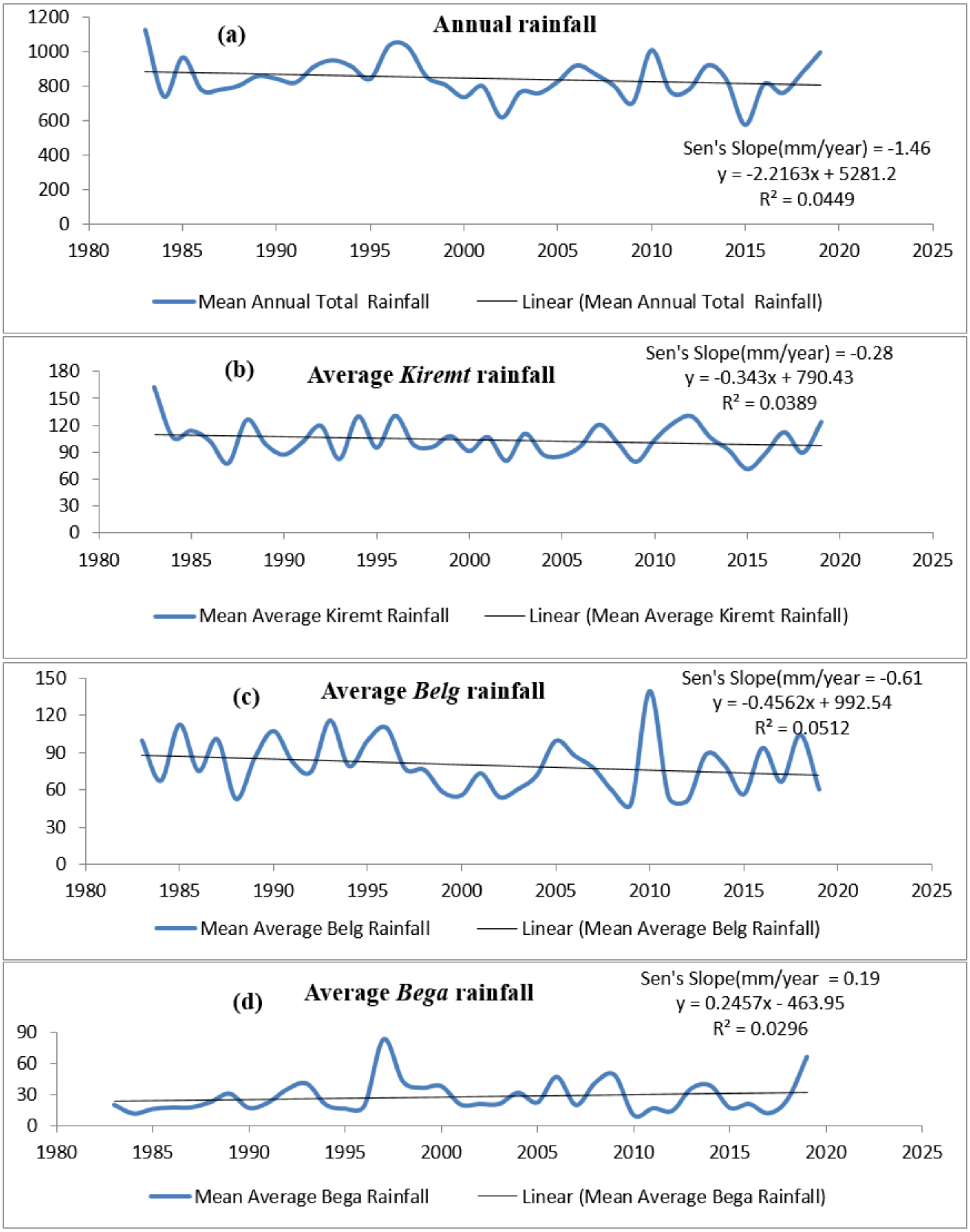

Figure 11

Long-term annual (a), and average Kiremt (b), Belg(c) and Bega (d) rainfall of West Harerge Zone (1983-2019)

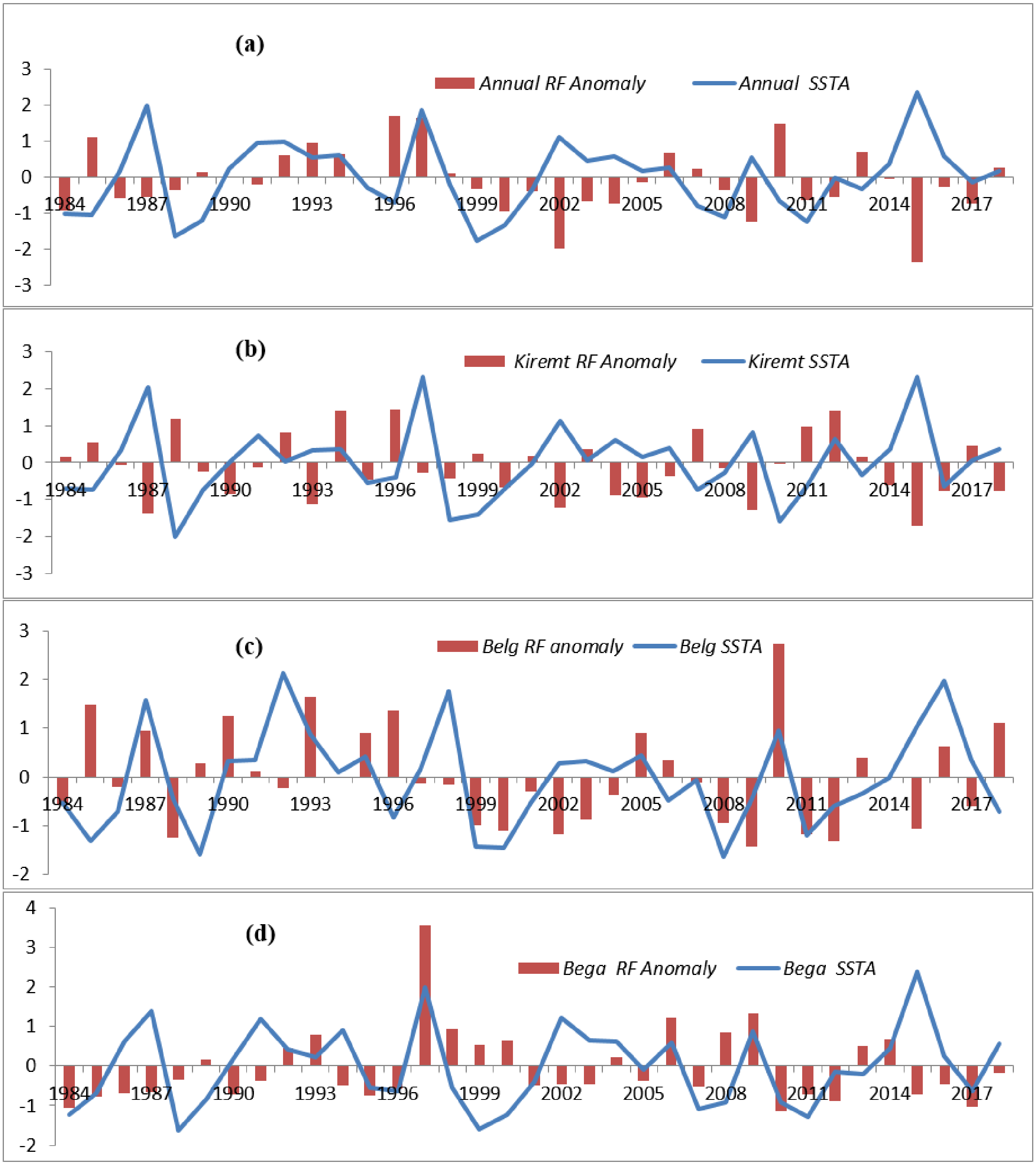

Figure 12

Association between annual rainfall anomaly and SST anomaly (a), Kiremt rainfall anomaly and SST anomaly (b), Belg rainfall anomaly and SST anomaly (c) and Bega rainfall anomaly and SST anomaly (d)

Supplementary Files